International Journal of Coal Geology 307 (2025) 104829

Contents lists available at ScienceDirect

International Journal of Coal Geology

journal homepage: www.elsevier.com/locate/coal

Fluvial architectural style and stacking patterns in a high-accommodation coal-bearing succession: the upper Permian Newcastle Coal Measures, eastern Australia

Christopher R. Fielding [a,*], Stephen McLoughlin [b], Chris Mays [c,d], Allen P. Tevyaw [e], Tracy D. Frank [a]

[a] Department of Earth Sciences, University of Connecticut, Beach Hall, 354 Mansfield Road (Unit 1045), Storrs, CT 06269, USA
[b] Swedish Museum of Natural History, Box 50007, S-104 05 Stockholm, Sweden
[c] Geology-Palaeontology Department, Natural History Museum Vienna, Burgring 7, 1010 Vienna, Austria
[d] School of Biological, Earth and Environmental Sciences, Environmental Research Institute, University College Cork, Cork, Ireland
[e] 2Blanding Avenue, East Providence, RI 02914, USA

ARTICLE INFO

Keywords:
Fluvial sedimentary facies
Coal geology
Palaeoclimate
Convergent tectonic volcanism
Sedimentation rate
Palynofacies

ABSTRACT

The upper Permian Newcastle Coal Measures (NCM) host world-class coal resources in coastal New South Wales, Australia. They formed close to the foredeep axis of a developing retroarc foreland basin associated with the Hunter-Bowen contractional event. In addition to the typical coal-bearing lithological suite of mudrocks, heteroliths, sandstones, and coals (with several beds of volcanic ash), the NCM preserve numerous, linear bodies of conglomerate up to 100 m thick and 20 km wide that are anomalous in the context of paralic coal-bearing successions worldwide. Four facies associations are recognized: A) linear bodies of conglomerate, gravelly sandstone and sandstone, interpreted as the deposits of major coastal plain channels, B) interbedded mudrocks and sandstones, interpreted as the product of coastal plain floodplains and floodbasins, C) coals and coaly mudrocks, interpreted as the product of coastal plain mires, and D) massive and bedded tuffs, interpreted as the product of pyroclastic falls and flows from nearby stratovolcanoes. Despite having formed on a coastal plain during a time of known sea-level changes, no depositional sequences can be recognized in the NCM, due to high rates of accommodation and sediment supply. The repeated co-occurrence of southward-trending major channel belts across the Newcastle coalfield is attributed to the area being located in the axial foredeep of the basin. A new palaeogeographic reconstruction is proposed in which the northern Sydney Basin, in the late Permian, extended further northwards across what is now the southern New England Orogen, and the north-south-elongate basin was drained by continental scale, basin-axial river systems that carried significant volumes of gravel.

1. Introduction

Since the 1980s, geologists have recognized the importance of accommodation as a control on coal formation and accumulation in sedimentary basins (Fielding, 1984, 1987; McCabe, 1991; Aitken and Flint, 1995; Hampson, 1995; Bohacs and Suter, 1997; Diessel et al., 2000; Shao et al., 2003; Wadsworth et al., 2003; Jerrett et al., 2011; Chalmers et al., 2013; Li et al., 2020, and many others). In paralic (coastal plain) domains, the prevailing view has been that fluctuations in sea level/base level are often a controlling factor on peat accumulation patterns, since such peats are formed within a few metres of sea level. A survey of peat accumulation rates from Holocene peatlands indicates that the rate of plant biomass production is often much greater than subsidence rates in all but the most rapidly subsiding basins. Accordingly, high accommodation settings are generally invoked to explain thick paralic coal deposits, although there is a limit imposed by the balance between accommodation rate, biomass production rate, and peat degradation (Bohacs and Suter, 1997; Diessel et al., 2000), with excessive rates of accommodation (perhaps associated with rising sea-level) giving rise to drowning of mires.

Within the suite of paralic coal-bearing successions, it is also recognized that there is a spectrum of variation in coal thickness and

* Corresponding author.
E-mail address: christopher.fielding@uconn.edu (C.R. Fielding).

https://doi.org/10.1016/j.coal.2025.104829
Received 26 February 2025; Received in revised form 17 June 2025; Accepted 17 June 2025
Available online 18 June 2025
0166-5162/© 2025 Elsevier B.V. All rights are reserved, including those for text and data mining, AI training, and similar technologies.

extent related to sediment supply rates, with higher rates of clastic sediment dispersal acting against formation of thick and, particularly, areally extensive peat/coal bodies (Fielding, 1985). There are few known examples of economically important paralic coal deposits associated with significant gravel-grade sedimentary rocks, since such lithologies are more commonly associated with small, rapidly subsiding, extensional or transtensional basins where subaerial fans issue either onto an alluvial surface or directly into standing water (e.g., Fielding, 1987; Jorgensen and Fielding, 1996; İnci, 2002).

The upper Permian Newcastle Coal Measures in the northern Sydney Basin, New South Wales, Australia Fig. 1), together with the partially coeval Illawarra Coal Measures and Wollombi Coal Measures in the southern and northwestern parts of the basin, respectively, constitute one of the world's largest bituminous coal resources, with an in situ coal resource estimated at 10,700 Mt. (Coal Resource Development Committee, 1994). The Newcastle Coal Measures are an example of an areally extensive, high-accommodation, coal-bearing succession with up to 12 mineable coal seams in a < 400-m-thick succession accumulated over ~3 m.y. (Fig. 2, Hawley et al., 1995). In addition to the typical coal measure inter-seam lithology suite of mudrocks and sandstones, together with volcaniclastic deposits, the Newcastle Coal Measures also preserve numerous bodies of conglomerate up to tens of metres thick, intercalated with coal seams. The processes that have collectively led to the formation and preservation of this unusual lithological assemblage have been debated at length, with little consensus.

The entirety of the Newcastle Coal Measures is encompassed by a single spore-pollen biozone, the *Dulhuntyispora parvithola* Zone (see review by Laurie et al., 2016), also informally called the 'Upper Stage 5'

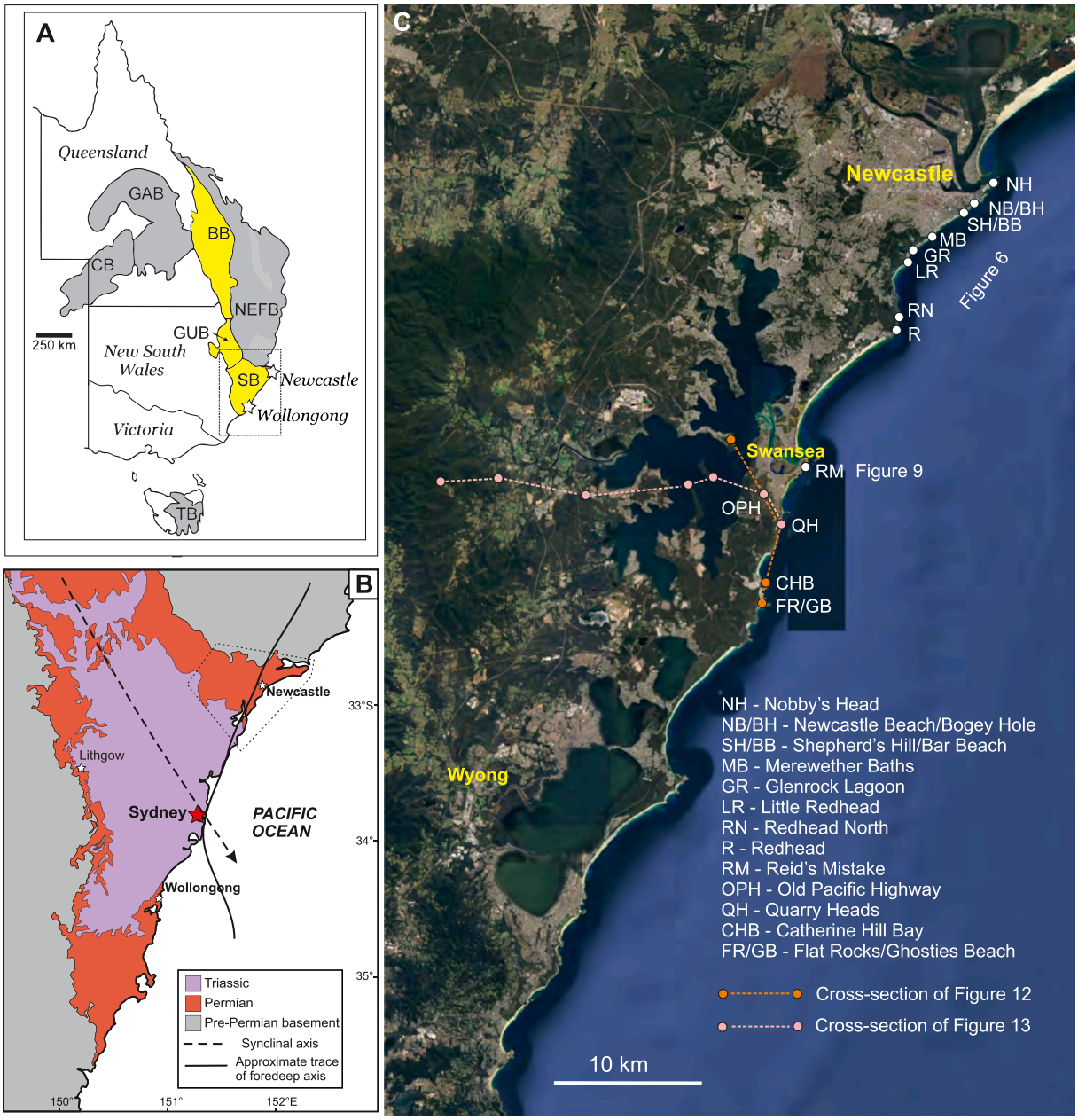

Fig. 1. Maps showing A) the meridional Bowen-Gunnedah-Sydney Basin System (yellow shade) in the context of Permian-Triassic sedimentary basins in eastern Australia, B) geology of the Sydney Basin of central coastal New South Wales, showing the southeastward-plunging synclinorium axis and north-trending foredeep axis as indicated by formation isopachs (Mayne et al., 1974), dashed outline indicates the Newcastle Coalfield, and C) satellite image of the Newcastle region showing the location of sites used in this study and of illustrated cross-sections (from Google Earth Pro, data from SIO, NOAA, U.S. Navy, NGA, GEBCO, image from Landsat/Copernicus). (For interpretation of the references to colour in this figure legend, the reader is referred to the web version of this article.)

Group	Ages	Formation	Coal Seams	Other named units
Narra-been	252.3 Ma			Munmorah Conglomerate
NEWCASTLE COAL MEASURES	252.8 Ma 252.7 Ma 252.9 Ma	Moon Island Beach	Vales Point Wallarah Great Northern	Karignan Conglomerate Cowper Tuff Mannering Park Tuff Teralba Conglomerate Booragul Tuff
	253.2 Ma	Awaba Tuff		Awaba Tuff
	253.4 Ma 254.2 Ma	Boolaroo	Fassifern Upper Pilot Lower Pilot Hartley Hill	Bolton Point Conglomerate Belmont Conglomerate Seahampton Sandstone Mount Hutton Tuff
		Warners Bay Tuff		Warners Bay Tuff
		Adamstown	Australasian Montrose Wave Hill Fern Valley Victoria Tunnel	Charlestown Conglomerate Stockrington Tuff Whitebridge Conglomerate Hillsborough Tuff Tingira Conglomerate Edgeworth Tuff Redhead Conglomerate Merewether Conglomerate
	255.0 Ma	Nobbys Tuff		Nobbys Tuff
		Lambton	Nobbys (Young Wallsend) Dudley Yard (West Borehole) Borehole	Signal Hill Conglomerate Cockle Creek Conglomerate Ferndale Conglomerate
	?255.5 Ma	Waratah Sandstone		Waratah Sandstone

Fig. 2. Stratigraphic column for the Newcastle Coal Measures (after Ives et al., 1999), showing available age constraints (see text for sources).

zone (Price, 1983) and later 'APP5' zone (Price, 1997). As noted by previous authors (Price, 1997; Shi et al., 2010), subdivisions of this zone in Eastern Australia have been stymied by the inconsistency of the few taxa that make their first appearances within this interval (e.g., *Dulhuntyispora spongia*, *Microreticulatisporites bitriangularis*), and/or due to uncertainties in the identification of informally named taxa used in some zonation schemes (e.g., '*Dulhuntyispora* sp. 205' or '*Dulhuntyispora dulhuntyi* (Form 296)' of Foster, 1979). The inability to palynostratigraphically subdivide the Lopingian of eastern Australia has been largely attributed to the remarkably long temporal span and consistent taxonomic composition of the late Permian glossopterid floral biome, which has been described as a 'climax community' (Fielding et al., 2022, p. 20). Nevertheless, these fossils provide a broad biostratigraphic framework facilitating correlation to other basins, and the analyses of palynological and macrofloral assemblages provide data aiding reconstruction of the palaeovegetation that generated the biogenic facies in these successions.

Here, we examine the sedimentology and stratigraphy of this rapidly accumulated succession of upper Permian (Lopingian), coarse clastic sedimentary rocks with thick coal seams in the northern Sydney Basin of eastern Australia. We provide details of architectural style among four facies associations representing four key components of a broad, lowland, coastal alluvial plain: major (trunk) channels, overbank environments (floodplains and floodbasins), coastal mires, and tephra-choked alluvial plain settings. These environments were somewhat affected by tidal modulation and backflow. We provide examples and illustrations of stratal stacking patterns, and use them to evaluate controls on sediment accumulation. We utilize a suite of recent, high-precision U—Pb CA-IDTIMS ages to assist in evaluating timescales of sediment accumulation, we reconstruct patterns of sediment dispersal, we plot isopachs of major tuff beds, and we integrate this information to propose a new palaeogeographic map for the depositional setting of the Newcastle Coal Measures and their southern equivalents in the Sydney Basin. In so doing, we seek to resolve some of the enduring controversies and misunderstandings surrounding this economically important succession, and show that thick, geographically extensive coal seams can form in direct association with large-scale, gravel-bearing, continental depositional systems.

2. The Newcastle Coal Measures of the northern Sydney Basin

The Newcastle Coal Measures (NCM) constitute the uppermost part of the Permian succession in the northeastern Sydney Basin of New South Wales (NSW), eastern Australia (Mayne et al., 1974; Harrington et al., 1989; Agnew et al., 1995). They accumulated in the axial foredeep of a retroarc foreland basin during the interval 255–252 Ma (late Wuchiapingian–Changhsingian: Figs. 1, 2). The Sydney Basin forms the southernmost onshore expression of the meridional Bowen-Gunnedah-Sydney Basin System, an elongate, interconnected Permian-Triassic basin complex that extends for up to 2000 km from north Queensland to southern NSW. The basin was located at high palaeolatitudes during the late Permian, though variably interpreted to have been situated at ~63–69°S (Torsvik and Cocks, 2013), ~65–75°S (Veevers, 2006) or ~ 85–90°S (Klootwijk, 2016). The Newcastle Coal Measures developed at the end of the ultimate, P4 glaciation of the Late Paleozoic Ice Age (Fielding et al., 2023) and coal accumulation terminated abruptly at the End-Permian Extinction (EPE) event (Metcalfe et al., 2015; Fielding et al., 2019, 2021), after which similar sedimentation patterns persisted but with an absence of peat-forming environments (Retallack et al., 1996; Fielding et al., 2021).

During and following late Permian–Triassic sediment accumulation, contractional deformation associated with the Hunter-Bowen Event (Holcombe et al., 1997; Glen, 2005; Rosenbaum, 2018) caused crustal shortening, propagation of thin-skinned thrust sheets westward from what is now offshore eastern Australia, and modification of the original Sydney Basin geometry such that the eastern basin margin is now largely obscured or incorporated into the southern New England Fold Belt (Fig. 1). Although the present-day synclinal axis of the Sydney Basin plunges to the southeast, isopach maps of late Permian (Lopingian) successions (Mayne et al., 1974) indicate that the original foredeep of the retroarc Sydney Basin trended slightly east of north and passed roughly along the present coastline in the vicinity of Newcastle, NSW. Thus, the Newcastle region, mined for its prolific coal resources for over 200 years, is located close to the original axis of the northern Sydney Basin foredeep (Fig. 1). Given an average thickness of ~400 m (e.g., Diessel, 1992 Fig. 7.9), the age range of the NCM indicates an approximate accumulation rate of 15 cm/1000 yrs. (not accounting for compaction; 34 cm/1000 yrs. accounting for compaction), which is rapid compared to the average (typically <5 cm/1000 yrs) for other retroarc foreland basins worldwide (Naylor and Sinclair, 2008; Allen and Allen, 2013).

The NCM preserve numerous volcaniclastic units distributed throughout the unit, ranging individually up to almost 30 m thick. These tuffs generally thin westward (inland from the present coast), and are interpreted to have been erupted from stratovolcanoes located in what is now the New England Fold Belt and offshore to the east (David, 1907; Mackenzie and Britten, 1969; Diessel, 1980, 1992; Creech, 2002; Chapman et al., 2022). Many of these tuffs are well-known to miners and geoscientists. They constitute excellent stratigraphic markers, being both distinctive in outcrop or underground workings, and more recently,

having been dated by high-precision geochronological methods (Huyskens, 2014; Metcalfe et al., 2015; Laurie et al., 2016; Nicoll et al., 2017; Fielding et al., 2019, 2021).

The NCM also preserve numerous fossil stump horizons and other dispersed woody debris that, locally, are sufficiently abundant to have influenced sediment deposition. Some of these so-called "fossil forest" horizons have been known since the 19th century (e.g., Clarke, 1843). Many occur at the base of volcaniclastic units, such as at Reids Mistake (Swansea South Heads: David, 1907; Loughnan and Ray, 1978; Diessel, 1984, 1992), and preserve in situ tree stumps encased in tuff and tilted in the direction of inferred sediment transport (e.g., Diessel, 1984). The unit also hosts abundant but low-diversity assemblages of leaves, reproductive organs, and roots derived predominantly from glossopterid gymnosperms (Supplementary Fig. 1). These are preserved extensively in floodbasin shales and immature palaeosols, and constitute the bulk of the organic matter in the rich coal resources within the unit. A rich insect fauna is also preserved in a few beds within the NCM (Jell, 2004; Shi et al., 2010) and invertebrate burrows are locally preserved in coastal facies (Herbert, 1997) but the unit, otherwise, contains few animal fossils (Warren, 1997). Palynology has been used for environmental interpretation and regional correlation of Sydney Basin upper Permian strata, particularly for beds close to the EPE horizon, in which there are abrupt changes in the spore-pollen assemblages (Helby, 1973; Mays et al., 2020; Vajda et al., 2020; Amores et al., 2025). However, Lopingian palynofloras of eastern Australia are otherwise relatively uniform with few prominent incoming, outgoing or hyperabundant taxa to facilitate biostratigraphic subdivisions of the upper Permian succession (Price, 1983, 1997; McMinn, 1987; Shi et al., 2010). This floristic uniformity suggests a relatively stable palaeoclimate, and this is supported by low variability in $\delta^{13}C_{org}$ and Chemical Index of Alteration (CIA) values in the Sydney Basin prior to the EPE (Fielding et al., 2019; Frank et al., 2021).

Here, we provide detailed sedimentary facies and palynofacies analyses of the NCM, while placing the outcrops into a biostratigraphic framework. This provides the broader sedimentological context of the NCM fossil forest horizons and the coal deposits with which they are associated. A detailed analysis of the vegetation stature, floristics, plant age classes, and local depositional settings of these fossil forests will be published elsewhere. Our sedimentological analysis provides implications for the environmental health of late Permian coal-forming terrestrial ecosystems in the 3 m.y. prior to the EPE.

3. Materials and methods

Palynological data derive from three outcrops of the Newcastle Coal Measures, northern Sydney Basin: 1, Murdering Gully/Merewether (32°57′36.39″S, 151°44′26.32″E); 2, Little Redhead (32°58′3.62″S, 151°44′16.07″E); and 3, Swansea South Heads (33° 5′47.21″S, 151°39′38.13″E). Two sedimentary rock samples were collected from each locality; these corresponded to facies B2, C1 or C2 (see Supplementary Table 1 for specifics). Five tablets of *Lycopodium clavatum* spores were added to each sample (manufactured by the Department of Geology, University of Lund, Sweden) prior to inorganic mineral digestion with hydrochloric acid followed by hydrofluoric acid. From each sample, two residues were produced. Kerogen residues, which underwent no sieving, heavy liquid separation or oxidation, were the subjects of palynofacies and organic microfossil concentration data collection. Oxidized residues, which underwent oxidation with Schulze's solution (a mix of $KClO_3$, H_2O, and NHO_3) and sieving with a 5-μm mesh to remove fine particles, were analyzed for biostratigraphic index taxa and alga/acritarch indicators of aquatic conditions. All residues were strew-mounted on glass coverslips, then sealed to glass slides with epoxy resin. Palynology samples were processed by Global Geolab Limited (Medicine Hat, Canada).

Concentration data of total terrestrial organic microfossils (TOMs)—which include all wood, leaves, plant spores, pollen, fungi and fossil resin—were collected with two distinct methods: the 'linear method' (Benninghoff, 1962; Stockmarr, 1971) and the 'field-of-view subsampling (FOVS) method'; see Mays et al. (2025) for details of these methods. Given their consistently lower error values, all concentration estimates presented in the text were from the FOVS method. All concentration estimates were conducted with fields-of-view sizes (at 630× magnification), and only grains ≥5 μm in diameter were counted; specimens smaller than this could not be identified consistently. To achieve parallel relative abundance data and linear method concentrations, palynofacies counts consisted of the following two criteria: 1, ≥500 grains; and 2, ≥ 3 *Lycopodium* spores. Palynomorph counts (consisting of all plant spores, pollen, algae and fungi) were conducted for biostratigraphic indices and algal populations. Target palynomorph count sizes were ≥ 300. Only one sample (S028838) failed to reach this count target. See Supplementary Table 1 for details of samples, *Lycopodium* tablets and count data.

Transmitted light microscopy and photomicrography of organic microfossils were conducted with a Zeiss Axioskop 2 transmitted light microscope equipped with a Canon EOS 700D camera. Residues and slides have been given the prefix 'S' and are housed at the Department of Palaeobiology, Naturhistoriska riksmuseet (NRM), Stockholm, Sweden.

Concentrations of Ba and Sr in mudrock were determined using a Bruker Tracer 5 g portable x-ray fluorescence (XRF) analyzer calibrated with a series of mudrock standards characterized by Rowe et al. (2012) and in-house reference materials. Samples were analyzed four times using a Bruker Tracer 5i in the Sedimentary Geology and Geochemistry Laboratory at the University of Connecticut, once under low-energy and once under high-energy conditions with different filters, to target a series of overlapping Kα ranges and enable precise analysis of relatively light and heavy elements. Ba was analyzed with no filter at 15 kV and 15 μA and a count time of 30 s. Sr analyses were undertaken at 50 kV with a Cu 100 μm:Ti 25 μm:Al 200 μm filter. In general, for the instrument used in the present study, the raw count rate per second (rcps) signals lay between 20,000 and 100,000 rcps.

The Sr/Ba palaeosalinity proxy developed by Wei and Algeo (2020) is based on a compilation of modern aqueous and sedimentary chemical data, demonstrating a relationship between the adsorption of dissolved species and salinity. It is particularly suitable for carbonate-poor mudrock and shale, as characterize the samples herein. However, its accuracy (~66 %) is somewhat limited due to the mobility of Sr and Ba during burial diagenesis, making it less reliable when used in isolation. In this study, the proxy is interpreted alongside palynological and sedimentological data to provide a more robust palaeoenvironmental assessment.

4. Results

4.1. Facies analysis

Several previous sedimentological analyses and facies schemes for the NCM have been compiled. This is unsurprising, given the excellent coastal exposures stretching for 35 km south from Newcastle city centre to Frazer Beach and the plethora of subsurface core data available. The comprehensive early work of David (1907) was followed by contributions by Loughnan (1966), Engel (1966), Duff (1967), Mackenzie and Britten (1969), Branagan & Johnson (1970), Conolly and Ferm (1971), Diessel (1980, 1992), Herbert (1997), and Lindsay and Herbert (2002). A further body of research has been presented in conference proceedings (e.g., Warbrooke, 1984, 1987; Diessel, 1986, 1989; Bocking et al., 1988) and in degree theses at the University of Newcastle (NSW: e.g., Warbrooke, 1981; Little, 1998; Creech, 2007), but not extensively published in the peer-reviewed literature. A series of field guides have been published, containing many details of unpublished or partly published studies (e.g., Eds. Herbert & Helby, 1980; Branagan & Diessel, 1992; Bamberry & Herbert, 1996). Nearly all of these works have concluded that the NCM are the products of sediment accumulation in coastal,

alluvial plain depositional environments crossed by large rivers draining an emerging orogen to the north and east, and flanked by extensive peat mires. Despite this plethora of previous work, however, consensus on the sedimentology and stratigraphy of the Newcastle Coal Measures has remained elusive.

More recently, Breckenridge et al. (2019), Maravelis et al. (2020), and Melehan et al. (2021) published facies and sequence stratigraphic analyses of the NCM, in which they re-advocated for a progressive upward regressive trend from lower delta plain to coarse-grained alluvial plain deposits (originally proposed by Engel, 1966). Breckenridge et al. (2019) further suggested that the upper delta plain and alluvial plain facies suites are separated by a regionally extensive erosion surface that they interpreted to be a major sequence boundary. Fielding et al. (2021) conducted a facies analysis of the uppermost NCM and overlying lowermost Narrabeen Group (Lower Triassic) and pointed out that the erosion surface of Breckenridge et al. (2019) is illusory, the purported contact being at multiple stratigraphic levels in the suite of exposures they examined (their Fig. 19). Rather than there being a single, abrupt upward change from sandstone-dominated delta plain deposits to conglomeratic alluvial plain deposits as advocated by Breckenridge et al. (2019), Fielding et al. (2021) showed that conglomerate- and sandstone-filled alluvial channel bodies are present at multiple levels in the NCM, and indeed a plethora of prior work indicates that such patterns prevail throughout the NCM, regionally (e.g., Diessel, 1980; Agnew et al., 1995; Boyd et al., 1998; Lindsay and Herbert, 2002).

Furthermore, the ages presented by Maravelis et al. (2020), their Fig. 10) formed the basis for a reinterpretation of the stratigraphy in which they argued that three tuffs from different parts of the NCM (from which they derived comparable ages) are in fact coeval with each other and imply simultaneous accumulation of disparate sections of the NCM. This extraordinary proposal is inconsistent with over 200 years of accumulated experience and data from the coalfield, including: 1. geological mapping that demonstrates progressive southward younging; 2. a plethora of surface and underground mine workings together with coastal outcrops that have led to the recognition of a detailed stratigraphy with up to 12 coal seams each of which has a distinctive internal stratigraphy; 3. fully cored boreholes that verify this stratigraphy and the overall thickness of the NCM; and 4. a suite of previously published and unpublished ages that are internally consistent with each other and that are widely accepted (cited in Fig. 2). The ages presented by Maravelis et al. (2020) are, in contrast, internally inconsistent with each other, insofar as strata higher in the stratigraphy are apparently older than others from lower in the stratigraphy (Fig. 10 of Maravelis et al., 2020). Their Fig. 5A, which illustrates representative zircons analyzed from tuff samples, shows only a strew of mineral grains of unknown composition or origin, and there are no cathodoluminescence images to justify the choice of grains analyzed (either in the main document or in the Supplementary file). The age spectra are of low quality, with few data points lying within the weighted mean interpretation, and with values outside of that range both above and below in some cases. On this basis, we judge the ages reported by Maravelis et al. (2020) to be unreliable and their stratigraphic reinterpretation to be unjustified.

Below, we document a new facies analysis of the NCM, in which we recognize four Facies Associations, each composed of multiple facies. Facies Association A (FAA; Fig. 3) comprises conglomerate- and sandstone-filled, mainstem (trunk) channel bodies <20 km wide and with elongate plan geometry (e.g., Fig. 5 of Fielding et al., 2021). Facies Association B (FAB; Fig. 4) consists of interbedded sandstones and mudrocks at various scales, interpreted to record overbank environments ranging from channel-proximal levee and splay facies to more distal floodplain and floodbasin deposits. Facies Association C (FAC; Fig. 5) consists of organic-rich deposits (coal, coaly shale, and associated organic-rich mudrocks, sandstones, and breccias) of interpreted mire origin, and Facies Association D (FAD; Fig. 5) comprises an array of volcaniclastic deposits that collectively record periods when the depositional surface became choked with primary and reworked volcanic ejecta from nearby explosive rhyodacitic eruptions. Overall, the depositional environment of the Newcastle Coal Measures is inferred to have been an extensive, rapidly subsiding, coastal alluvial plain, affected by tidal backflow and by the products of nearby, explosive volcanic eruptions on several occasions.

4.1.1. *Facies Association A (FAA) – major channel deposits*

Description. FAA consists of erosionally based bodies of pebble to cobble conglomerate, clast-rich sandstone, and sandstone <50 m thick, locally punctuated by minor mudrock and tuff partings (Table 1, Fig. 3). Thicker bodies are multistorey, with individual storeys typically 10–15 m thick (but in at least one case, the Redhead Conglomerate, at least 42 m thick). Composite Facies A1 bodies up to 100 m thick have been identified by subsurface mapping (Bocking et al., 1988). Individual bodies have been mapped by multiple researchers and found to describe mainly south to southwest-directed, linear belts up to 20 km wide (Branagan and Johnson, 1970; Bocking et al., 1988; Diessel, 1992; Lindsay and Herbert, 2002; Fielding et al., 2021).

Three component facies are recognized. Facies A1 comprises the conglomeratic channel fills (Table 1). Conglomeratic bodies and storeys are typified by complex interbedding of conglomerate, clast-rich sandstone, and sandstone but, nonetheless, dominated by pebble- to cobble-grade polymict ortho- and para-conglomerate (e.g., Fig. 3A, B, E). Various current-generated sedimentary structures are preserved (Table 1). Storey boundaries are defined by laterally persistent erosion surfaces with >1 m of erosional relief, that commonly truncate discontinuous partings of finer-grained lithologies (e.g., Fig. 3G). Facies A2 comprises sandstone-dominated bodies of similar geometry to Facies A1, commonly in complex interbedded relationships with Facies A1 (e.g., Fig. 3B, E, F) and, in many cases, located towards the lateral margins of major conglomerate bodies (e.g., Fielding et al., 2021 Fig. 6). Some Facies A2 bodies are also multi-storey, with individual storeys similar in thickness to those of Facies A1 (e.g., Fig. 3C, D). Overall, the architecture of Facies A2 bodies is nearly equivalent to that of Facies A1, although it is also true that the average thickness of Facies A2 bodies is less than that of Facies A1, giving the impression that they are deposits of somewhat lower stream rank. Facies A3 is defined to account for mainly sandstone bodies with bimodal to bipolar palaeocurrent distributions, increased evidence for bioturbation, and preservation of rhythmically laminated mudstone partings and synaeresis cracks.

Notable features common to all three FAA facies are the preservation of macroform foreset bedding in sets up to 40 m thick (but more commonly <15 m; Fig. 3A), the presence of mesoform upper flow regime stratification, particularly antidunal stratification, and the presence of upright, in situ, tree stumps and trunks preserved within the conglomerate or sandstone bodies (e.g., Fig. 3F). The dip directions of macroform foresets are typically aligned at 60–120 degrees to those of mesoform structures preserved in the same body (Fig. 6). Crude planar and low-angle stratification is common in Facies A1, along with locally-recognized examples of antidunal stratification. The latter is more prevalent in Facies A2 and A3, however, where it is easier to recognize. At one locality (Ghosties Beach), a train of large antidunes is preserved as an aggradational form set in a Facies A2 lower storey of the Karignan Conglomerate (Fielding et al., 2021 Fig. 7A).

Interpretation. FAA is interpreted as the deposits of alluvial channels and channel belts that crossed a broad, coastal alluvial plain. In this context, Facies A1 is interpreted as the thalweg deposits of 10–40-m-deep channels with varying sinuosity. Facies A2 is interpreted to record portions of channel fills formed during periods of dominantly sand supply, and Facies A3 to represent such channel fills that were located within the coastal alluvial zone (or backwater zone) under the influence of tidal backflow and influx of brackish water. Many channel bodies are composite, multistorey entities with individual storeys commonly dominated by one facies. The abundance of upper flow regime stratification, and of upright, in situ tree fossils in FAA deposits, is interpreted to record channels that experienced high levels of discharge variability

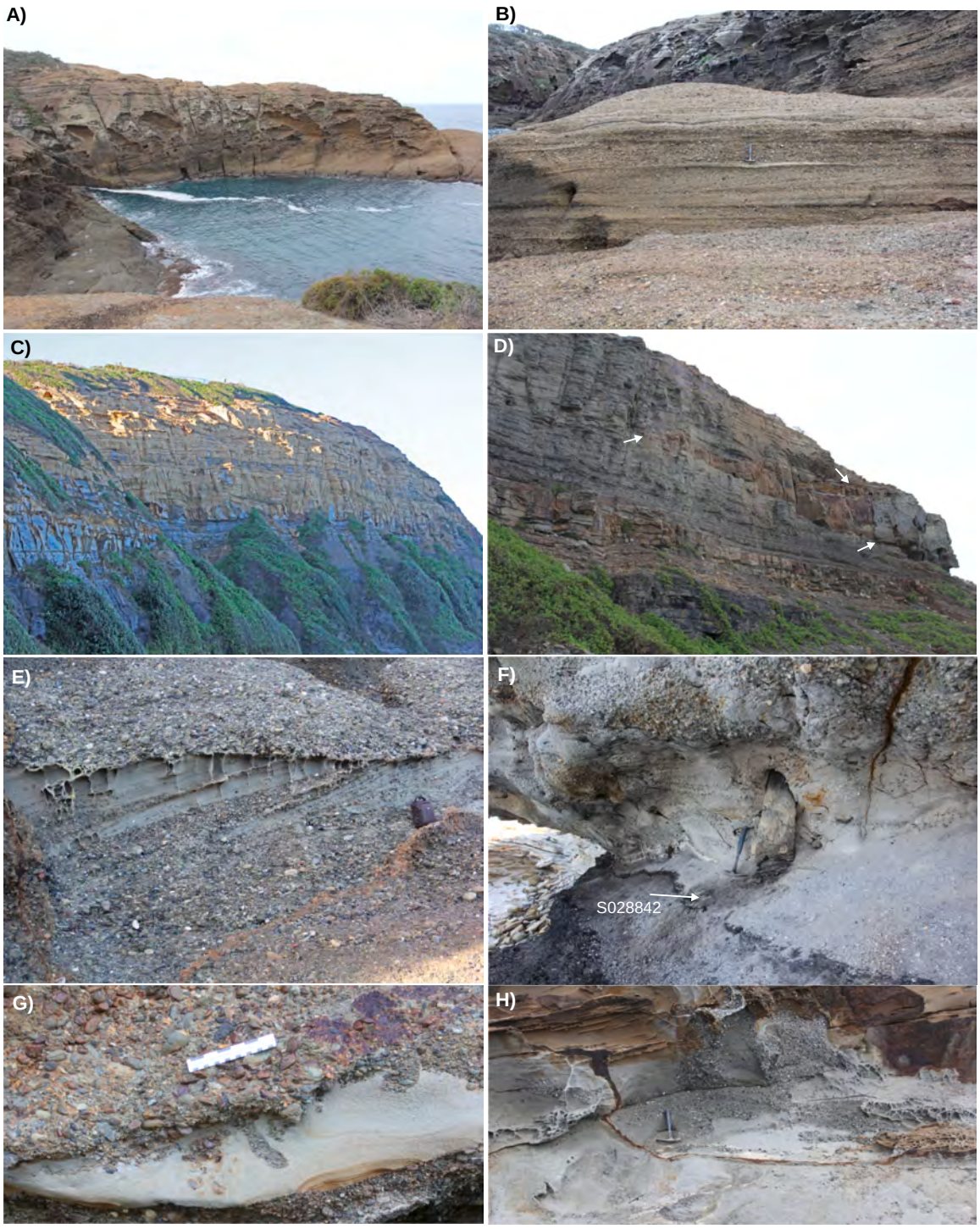

Fig. 3. Field photographs of Facies Association A (Major Channel Deposits). A) View of Upper Teralba Conglomerate at Shark Hole north of Catherine Hill Bay, showing macroform cross-set overlain by flat-lying, topset strata. The cross-set is at least 17 m thick and is interpreted from palaeocurrent relationships to be a lateral accretion set associated with migration of a fluvial point bar. B) Close-up view of the body shown in (A), showing macroform beds in strike section (flat-lying) and mesoform cross-bedding dipping to the left, verifying the lateral accretion interpretation. Hammer for scale is 0.25 m. C) View of coastal cliff at Shepherd's Hill, Newcastle, showing the multistorey nature of the Signal Hill Conglomerate (21 m thick) with sandstone-dominated storeys separated by fine-grained partings. D) Coastal cliff at Little Redhead north end, showing southward pinchout of the Merewether Conglomerate (white arrows). Victoria Tunnel Seam visible at base of exposed section, which is about 35 m thick in total. E) Close-up view of cross-bedding in interbedded conglomerate and sandstone, Karignan Conglomerate north of Birdie Beach. Instrument case is 0.20 m high. F) Close-up view of upright, in situ fossil tree trunk encased in the basal 1 m of the Belmont Conglomerate at Reids Mistake, south end. Note the abundance of coalified plant trash preserved in the vicinity of the axis. Hammer 0.25 m for scale; arrow indicates sampling point of palynology assemblage S028842. G) Close-up view of sandstone parting in Facies FA1 conglomerate in the Upper Teralba Conglomerate north of Catherine Hill Bay. Note the conglomerate-filled load casts and burrows subtending into the sandstone parting (below scale card, 0.15 m). H) Sedimentary intrusions of conglomerate into sandstone of the Upper Teralba Conglomerate at Quarry Head. Vertical pipes and subhorizontal sills are visible to the right of the hammer (0.25 m).

Fig. 4. Field photographs of Facies Association B (Overbank Deposits). A) Thick succession of Facies Association B deposits at Redhead (below Victoria Tunnel Seam, visible near top of field of view). The mudrock-dominated lower part of the section (Facies B2 and B3) passes upward into more rhythmically-interbedded and sandstone-dominated Facies B1. Geologist for scale 1.70 m. B) Close-up of Facies B1 below Yard Seam at Shepherd's Hill, showing rhythmically-interbedded sandstone and mudrocks. Sandstones are internally dominated by climbing ripple cross-lamination and soft-sediment deformation structures, suggestive of rapid deposition. Notebook is 0.20 m high. C) View of minor channel margin in Facies Association B deposits south of Merewether Baths below the Dudley Seam (also exposed). The channel shown is part of a multilateral complex of apparently coeval minor channels, interpreted to record the proximal reaches of a crevasse splay minor delta. Hammer (circled) 0.25 m. D) Close-up view of an upright, in situ fossil tree stump with basal flare passing through another Facies B2 minor channel sandstone body, same locality as for (C). The tree was rooted into the substrate below the channel body, suggesting that it predated formation of the channel and protruded through the channel while it was being formed and filled. Hammer (circled) 0.25 m. E) Close-up view of sedimentary dykes subtending from the base of a minor channel shown in (C) into underlying Facies B2. Hammer 0.25 m. F) Close-up view of rhythmically bedded (white arrow) and cross-bedded sandstone-siltstone of Facies B3 showing backflow ripples migrating up the cross-bed foreset (black arrow). These bedding features collectively suggest a tidal backflow constituent to depositional process. G) View of a probable glossopterid trunk with radiating roots, preserved in situ in Facies B2 below the Victoria Tunnel Seam on the shore platform at Redhead. Hammer 0.25 m. H) Bedding plane preservation of a *Glossopteris* leaf mat in Facies B2 siltstone, Little Redhead, below the Victoria Tunnel Seam.

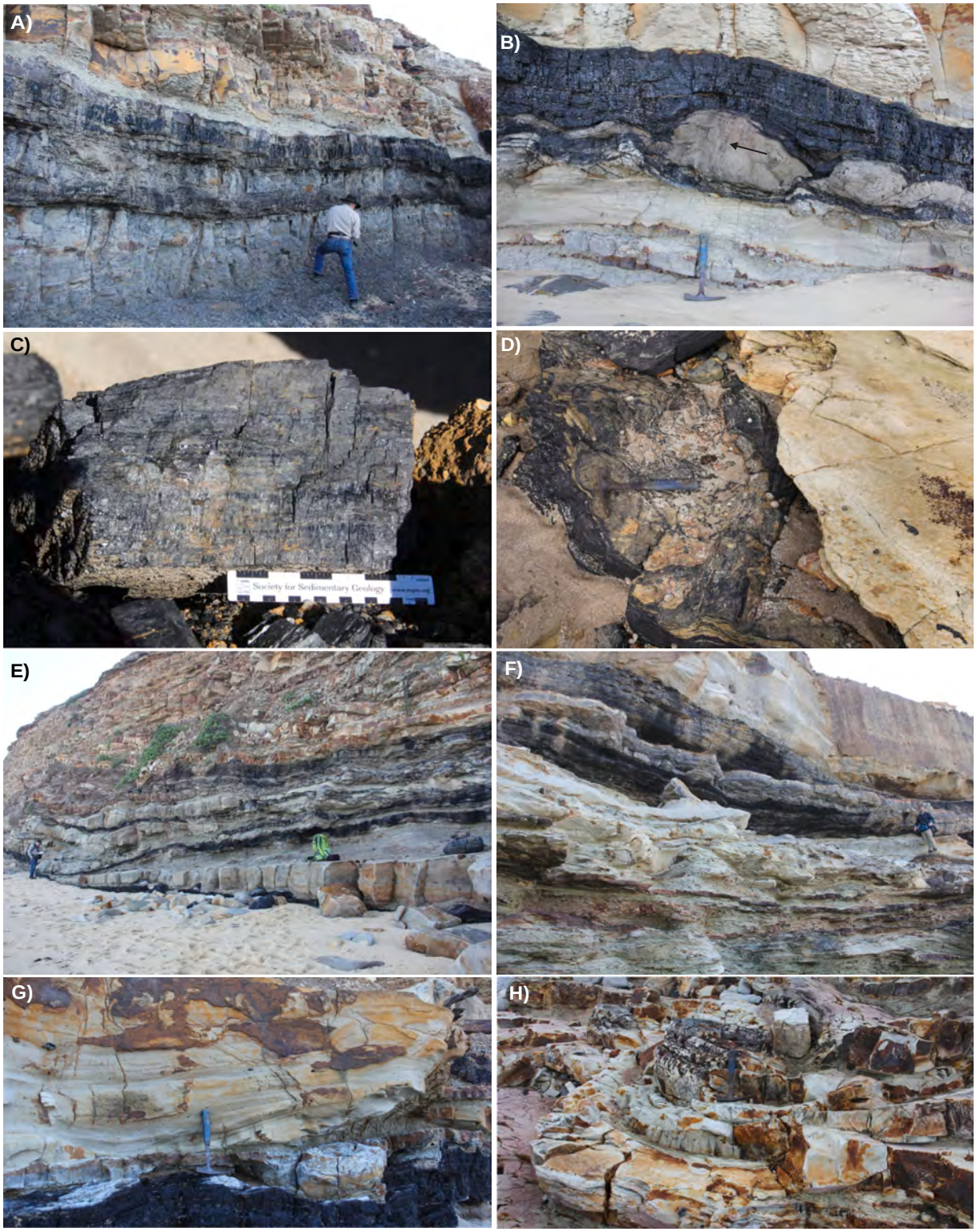

Fig. 5. Field photographs of Facies Associations C and D. A) Interbedded Facies C1 and C2 (Nobby's Seam) overlain by Facies D1 (Nobby's Tuff) at Glenrock Lagoon. Geologist 1.70 m for scale. B) Close-up view of the base of Nobby's Seam at Glenrock Lagoon, showing interbedding of Facies C1 and C2 with conspicuous *Vertebraria* roots below the main coal seam (arrowed). C) Fresh face of dull banded coal (Facies C1), Vales Point Seam at Wybung Head. Scale card 0.15 m. D) Bedding plane view of large, tubular glossopterid roots in the uppermost Lower Pilot Seam at Reids Mistake. Hammer 0.25 m. E) Complexly interbedded coal (Facies C1/C2) and tuff (Facies D1) of the Nobby's Seam and overlying Nobby's Tuff at Glenrock Lagoon. Geologist 1.70 m for scale. F) Chaotic tuff-filled channel body (cream-coloured central part of section) at Reids Mistake south end, below the Upper Pilot Seam. Geologist standing on channel fill, 1.70 m. G) Close-up view of upper flow regime stratification (flat and low-angle stratification, possible antidunal bedding) in the basal Nobby's Tuff at Glenrock Lagoon. Hammer 0.25 m. H) Upright, in situ tree stump surrounded by centroclinal cross-bedding in tuff (Facies D1), above Lower Pilot Seam at Reids Mistake. Hammer 0.25 m.

Table 1
List of facies identified in the Newcastle Coal Measures, and their classification into four Facies Associations.

Facies Association	Interpretation	Lithology	Sedimentary Structures and Fossils	Geometry
A	**Major Channel Deposits**			
A1	Gravelly Alluvial Channel Fills	Poorly to moderately sorted, matrix and clast-supported, locally erosionally based, pebble- to cobble- conglomerate bodies <50 m thick (individual storeys mainly <15 m thick, exceptionally <42 m); matrix is coarse- to very coarse-grained sandstone, conglomerates are polymicitic (jasper, quartzite, metasedimentary and volcanic clast types prevalent), first cycle pyroclastic, coal and intraformational siltstone clasts also common, and peat rafts. Discontinuous (< 3 m thick) medium- to very coarse-grained sandstone, mudrock, and tuff partings	Crude flat stratification, dune-scale cross-bedding (unimodal palaeoflow distributions), macroform cross-beds up to 17 m thick, local antidunal stratification, clast imbrication, injection features and soft-sediment deformation structures, in situ fossil tree stumps, wood adpressions, and petrified logs. Sandstone partings preserve ripple cross-lamination, planar stratification, soft-sediment deformation structures, and coaly traces. Rare bioturbation, BI = 0–1	Lenticular in cross-section, compensationally stacked, single- and multistorey bodies <50 m thick, ribbon-like in planform with lateral pinchout margins. Macroform foresets show slight upward convexity or sigmoidal profile
A2	Sandy Alluvial Channel Fills	Sharply based bodies of medium- to coarse-grained sandstone and pebbly sandstone, locally tuffaceous, < 25 m thick with lenses of extraformational gravel and intraformational siltstone clast breccia/ conglomerate, local mudrock partings	Trough cross-bedding (unimodal palaeoflow distributions), planar lamination, local internal erosional surfaces, antidunal stratification, injection features and soft-sediment deformation structures, in situ tree stumps, wood adpressions and petrified wood, finely disseminated plant debris, and coaly traces. No bioturbation, BI = 0	Lenticular in cross-section, compensationally stacked, single and multistorey bodies <10 m thick, ribbon-like in planform, pinchout lateral boundaries
A3	Tidally Influenced Coastal Plain Channel Fills	Erosionally-based bodies of fine- to medium-grained sandstone <10 m thick; fine-grained partings with rhythmically interlaminated siltstone-sandstone couplets	Trough cross-bedding (bimodal to bipolar palaeoflow distributions), rhythmic lamination, planar stratification, ripple cross-lamination, low-angle lamination, lenticular bedding, syneresis cracks, load casts, local root penetration, coaly traces, and bioturbation at tops of bodies; BI = 0–2, trace fossil assemblages includes fugichnia, navichnia, *Diplocraterion, Rosselia, Teichichnus, Planolites, Thalassinoides, Lockeia, Zoophycos*	Multistorey bodies <10 m thick, Plan geometry unverified
B	**Overbank Deposits**			
B1	Levee	Thinly and rhythmically interbedded siltstone and very fine- to fine-grained sandstone, intervals <4 m thick	Ripple cross-lamination and climbing ripple cross-lamination, sinusoidal ripples, flat lamination, minor small-scale cross-bedding, soft-sediment deformation, mudstone clasts, plant debris and coaly traces	Wedge-shaped in cross-section, located on the lateral margins of Facies Association A bodies
B2	Floodbasin deposits on a lowland alluvial plain	Heterolithic (interlaminated and thinly interbedded) very fine- to medium-grained sandstone and drab grey siltstone, intervals < c. 20 m thick, local sharp-bounded sandstone beds <0.5 m thick, short (< 1.5 m) coarsening-upward intervals, locally channelized sandstone bodies <1.8 m thick and 10s of m wide	Ripple cross-lamination, trough cross-bedding, flat lamination, load casts, siderite nodules, common pedogenic modification (slickensides, local red mottling, root penetration, *Vertebraria* casts), wood adpressions, disseminated plant debris, abundant spores and pollen, rare algae and acritarchs.	Sheet-like bodies lateral to Facies Associations A and B. Highly variable thickness but up to 18 m at channel boundaries. Bodies encase and vertically separate Facies A and B bodies
B3	Brackish-influenced Coastal Plain Floodbasin Deposits	Heterolithic (interlaminated to thinly-interbedded) very fine- to medium-grained sandstone and drab grey siltstone, intervals generally <20 m thick, local sharp-bounded sandstone beds <0.5 m thick, short (< 1.5 m thick) coarsening-upward intervals	Trough cross-bedding, ripple cross-lamination, flat lamination, rhythmic lamination, synaeresis cracks, mud drapes, load casts, root penetration, siderite nodules, *Vertebraria* casts, wood adpressions, disseminated plant debris, abundant spores and pollen, rare algae and acritarchs, BI = 0–2, trace fossil assemblages include fugichnia, navichnia, *Teichichnus, Planolites*	Lateral extent unverifiable. Vertically separates bodies of Facies Association C
B4	Lacustrine	Dark–light grey shale and siltstone with local interlaminated, very fine-grained sandstone, intervals <2 m thick	Finely laminated, sparse root penetration, macerated plant debris, *Vertebraria* roots, and locally well-preserved leaves of the *Glossopteris* flora. Rare, simple bioturbation, BI = 0–1	Spatially limited and only preserved in sections not affected by fluvial downcutting above uppermost coal seam
C	**Mire**			
C1	Mire	Coal in units 2–8 m thick, thicker intervals commonly with clastic and pyroclastic partings, local beds of organic-rich microbreccia	Compositional banding and stratification, some intervals massive, extremely abundant coalified plant debris and roots, minor spores and pollen, negligible algae/ acritarchs, no bioturbation, BI = 0	Sheet-like over several km. Coal seams split around Facies Association A, B, and C bodies
C2	Clastic mire	Interbedded coal, carbonaceous shale, mudrocks and minor sandstone, with local	Compositional banding and stratification, some intervals massive or soft-sediment-	Variable cross-sectional geometry

(*continued on next page*)

Table 1 (*continued*)

Facies Association	Interpretation	Lithology	Sedimentary Structures and Fossils	Geometry
		sedimentary breccias of plant fragments in a siltstone matrix	deformed, abundant coalified plant debris (including spores and pollen) and roots, very rare algae/acritarchs, no bioturbation, BI = 0	
D	**Pyroclastic Deposits**			
D1	Pyroclastic Fall and Flow Deposits	Tuff and tuffaceous sandstone, tuff clast sedimentary breccia	Massive to stratified (flat and undular stratification, local cross-bedding and ripple cross-lamination), some graded beds, soft-sediment deformation, plant roots, fossil tree stumps (upright or tilted), leaf fragments, coaly debris, petrified logs	Variable geometries including channel fills. Some bodies are sheet-like, whereas others thicken and thin laterally; local evidence of pinchout

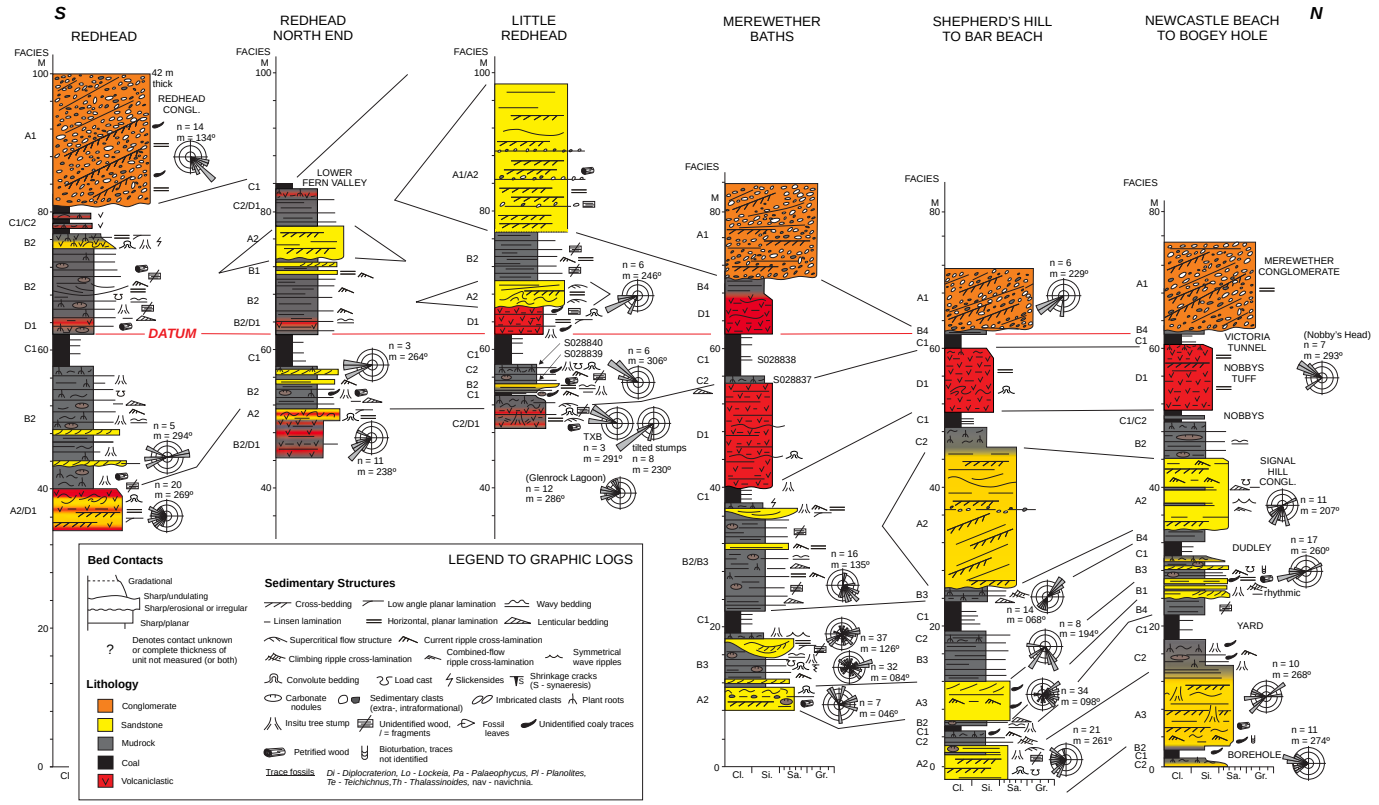

Fig. 6. North-south cross-section showing correlation of outcrop sections measured from Newcastle Beach in the north to Redhead in the south. Note the utility of major tuff beds as stratigraphic markers, and the lensoid nature of Facies Association A conglomerate/sandstone bodies, particularly the Merewether Conglomerate which becomes sandstone-dominated and then pinches out gradually to the south. Datum is the top of the Victoria Tunnel Seam.

on multi-year timeframes and where channel bar tops were periodically exposed or shallow enough to enable the establishment of large woody plants (Fielding et al., 2018, 2021, 2025). The high discharge variability motif was found by Fielding et al. (2021) to characterize the uppermost Permian section in the Sydney Basin but, herein, we recognize that alluvial style throughout the Lopingian NCM.

Channel planform is interpreted to have been variable, but commonly meandering, with many demonstrable examples of lateral accretion sets (macroform cross-sets up to 40 m thick; Fig. 6). Channel belts have been mapped as somewhat sinuous, linear tracts up to 20 km wide (e.g., Bocking et al., 1988; Lindsay and Herbert, 2002; Fielding et al., 2021) draining broadly southward, with demonstrable mapped examples of channel confluences (e.g., Fig. 5C of Fielding et al., 2021) indicating that at least some axially-draining fluvial systems were contributive in nature. Mapping indicates that, in flow-transverse cross-section, channel belt bodies were mostly stacked in a compensational (offset) pattern, and in places influenced by early compaction of underlying, thick peat bodies (cf. Van Asselen, 2011). The likely role of early peat compaction on the location and cross-sectional geometry of FAA bodies in the Newcastle Coalfield has been noted by several researchers (e.g., Flood and Brady, 1985; Diessel and Moelle, 1988; Bocking et al., 1988). Further, Branagan & Johnson (1970) noted a coincidence in orientation and location of thick, multistorey FAA bodies with mapped faults across the coalfield, suggesting local structural control.

4.1.2. *Facies Association B (FAB) – overbank deposits*

Description. FAB consists of four facies that are dominated by interbedded sandstone and mudrocks (Table 1, Fig. 4). These lithologies occur in irregularly shaped bodies in plan view and, in cross-section, are commonly in lateral contact (interfingering or erosional) with FAA facies. Facies B1 comprises rhythmically interbedded sandstone and siltstone at the cm to dm scale (e.g., Fig. 4B), and is found in close association with FAA facies. Facies B2 consists of intervals of more

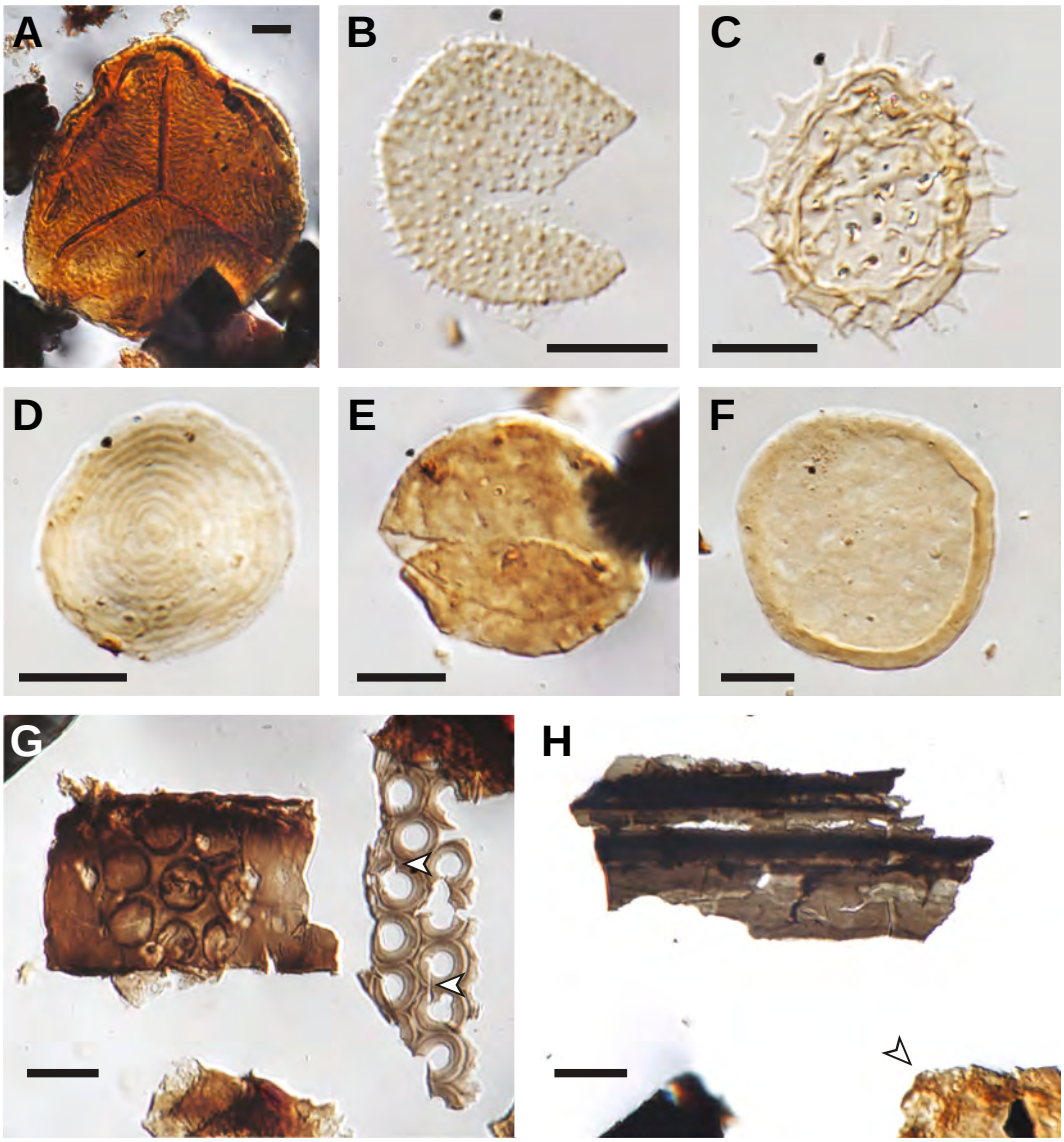

Fig. 7. Selected organic microfossils for biostratigraphic and palaeoenvironmental interpretations; slide numbers (#) and England Finder co-ordinates (EF) are in parentheses and in the format '#-EF', all scales = 10 μm. A, B) Index taxa of the *Dulhuntyispora parvithola* Zone; A, *Dulhuntyispora parvithola* (Balme and Hennelly, 1956a) Potonié, 1960, Murdering Gully/Merewether, S028837 (3-T26); B, *Micrhystridium evansii* Price, 1983, a mixohaline indicator for eastern Australian basins, Swansea South Heads, S028842 (1-Q39[4]). C) *Micrhystridium* sp., note the relatively elongated processes, typical of elevated salinity (e.g., Stricanne et al., 2004; van Soelen et al., 2018), Swansea South Heads, S028842 (1-V26). D—F) Algae (or putative algae) typical of the *Peltacystia* Microalgal Province (sensu Mays et al., 2021); D) *Circulisporites* (=*Chomotriletes*) *parvus* de Jersey, 1962, freshwater euglenophycean cyst (see van de Schootbrugge et al., 2023), Swansea South Heads, S028842 (1-U28); E) *Ovoidites scissus* (Balme and Hennelly, 1956b) Zavattieri et al., 2020, freshwater zygnematophycean alga, Little Redhead, S028839 (1-V25[2]); F) *Pilasporites calculus* Balme and Hennelly, 1956b, putative freshwater alga of unknown affinity, Swansea South Heads, S028842 (1-U8). G, H) Charcoalified wood; G) two gymnosperm (?glossopterid) tracheids, the partially charcoalified tracheid (right) can be distinguished from the non-charcoalified tracheid (left) by its slight discolouration and fractured oval pit borders (arrows); H) severely charcoalified tracheid, expressed by the numerous fractures and absence of colour compared to a non-charcoalified phytoclast (arrow).

variably interbedded sandstone and mudrocks with sheet-like, sharp-bounded sandstone beds up to 0.5 m thick, erosionally-based/laterally restricted and channelized sandstone or heterolithic units up to 3.0 m thick, and short (< 1.5 m thick) coarsening- and thickening-upward cycles (Fig. 4A, C). The palynofacies assemblages from Facies B2 are dominated by fossil leaf and wood fragments (58–77 %). Miospores (plant spores + pollen) were far more abundant (14.9–32 %) in Facies B2 than any other facies examined here. Similarly, the remains of algae and acritarchs, although rare (1.1–1.6 %), were more abundant than in any other facies. Terrestrial organic microfossil concentrations for Facies B2 are moderately high (c. 7.4×10^5–$2.6 \times 10^6 \pm 14.8$–18.1 % fossils/g). Facies B3 is similar lithologically to Facies B2 but contains a taxonomically limited suite of trace fossils (typically *Planolites* and navichnia) and also preserves synaeresis cracks, mud drapes (including paired mud drapes), and rhythmic interlamination structures. Facies B4 comprises laminated fine-grained mudrocks with variable interlaminated sandstone content, generally as mudrock-dominated heterolithes. All four FAB facies preserve an array of mostly ripple-scale physical structures (e.g., Fig. 4F), together with common soft-sedimentary structures (e.g., Fig. 4E).

All four FAB facies (but especially B2 and B3) have in common that they preserve both ex situ (transported) and in situ plant fossils in abundance, including large, complex root systems of glossopterid trees typically assigned to the fossil-genus *Vertebraria* (e.g., Fig. 4G). Some discrete, ~1-m-thick intervals exposed on coastal platforms host large numbers of in situ roots and stumps at the same stratigraphic level,

spaced 1–3 m apart. Upright or inclined, in situ fossil trees are also common dispersed within thinly interbedded Facies B2 and B3, and even passing through the entirety of FAB channelized sandstone bodies, for example below the Dudley seam south of Merewether Baths (Fig. 4D). Beds rich in matted leaves of *Glossopteris* (Glossopteridales) and *Noeggerathiopsis* (Cordaitales) (Supplementary Fig. 2A), and less abundant axes of *Paracalamites* (Sphenopsida), are also common (e.g., Fig. 4H).

Interpretation. FAB is interpreted as the deposits of overbank environments that flanked the coastal fluvial channel deposits of FAA, on the basis of their finer-grained lithologies and geometrical relationships. Thickly, and in many cases, rhythmically interbedded sandstone and siltstone intervals are interpreted as proximal overbank deposits that likely formed levees adjacent to fluvial channels. Some continuous cliff exposures, such as at Redhead north, demonstrate directly the genetic association between FAA and Facies B1. Large, surface mine exposures of some ancient successions have conclusively shown regularly interbedded facies similar to this as being the product of levees in direct contact with channel margins (e.g., Pennsylvanian of NE England, Fielding, 1986 Fig. 9; Permian of Queensland, Australia, Fielding et al., 1993 Fig. 9). Sharp-bounded sandstone beds in Facies B1, in many cases, record individual overbank flow events from adjacent rivers, as has been established from studies of modern levees (e.g., Ferguson and Brierley, 1999; Bridge, 2003). However, Filguera-Rivera et al. (2007) showed that levees can accrete both from "front-loading", i.e., sediment supplied diffusively from the channel during overbank floods, and from "back-loading", i.e., advective movement of sediment through floodbasins back towards the distal margin of the levee. Accordingly, some beds that thicken in the opposite direction to sharp-bounded sandstone beds in Facies B1 may be the product of levee backloading.

Facies B2 records various sub-environments within what were likely shallow floodbasins distal to levees, similar to those documented from the modern Cumberland Marshes in Canada by Perez-Arlucea and Smith (1999) and Farrell (2001). Using these analogies, mudrock-dominated variants of Facies B1 record portions of floodbasins distal to coarse sediment supply. Tabular, sharp-bounded sandstone beds likely record splay deposits from overbank flows derived from nearby channels. Short (< 2-m-thick) coarsening-upward sequences are interpreted to record progradation of shallow crevasse deltas, such as form after repeated flows into floodbasins through nearby channel bank breaches (crevasses; Perez-Arlucea and Smith, 1999; Bristow et al., 1999). Erosionally based, minor channel sandstone bodies are similarly interpreted to record the proximal portions of crevasse sub-delta feeder systems which, in modern analogues, are conspicuously channelized (Perez-Arlucea and Smith, 1999; Bristow et al., 1999; Farrell, 2001). Although the terrestrial microfossil concentrations in Facies B2 are moderately high, they are generally lower than in other facies, especially Facies C1 (mire deposits). This is likely a consequence of sediment dilution of fossil-rich mudrocks with fossil-poor sandstone. Organic-walled microplankton were represented by both saline/brackish acritarchs (*Micrhystridium*, Fig. 7B, C), freshwater zygnematophycean algae (e.g., *Ovoidites scissus*, Fig. 7E), freshwater cysts of probable euglenoid affinity (*Circulisporites [=Chomotriletes] parvus*, Fig. 7D; see discussion by van de Schootbrugge et al., 2023), in addition to putative algal groups that cannot be easily assigned environmental preferences (e.g., *Pilasporites calculus*, Fig. 7F). The combination of predominantly terrestrial plant remains and freshwater algae and euglenoids with marine acritarchs is suggestive of brackish conditions. A predominance of brackish conditions is also consistent with incidences of rhythmic interlamination structures, paired mud drapes, restricted trace fossil assemblages, and Sr/Ba ratios from mudrock samples of three drillcores through the NCM (Fig. 8). That such ratios characterize the entire NCM indicates that the basin remained in the backwater zone for much if not all of its history.

Facies B3 is interpreted to represent the same style of deposition as Facies B2, with the caveat that it shows evidence of formation under brackish groundwater and standing water conditions, and under the influence of tidal circulation, presumably within the backwater zone of

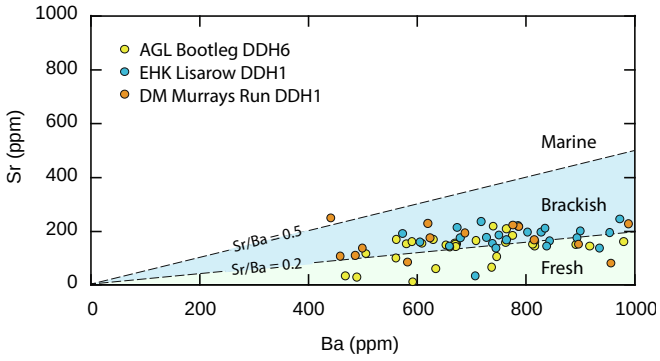

Fig. 8. Palaeosalinity estimates for mudstones in the Newcastle Coal Measures recovered in cores AGL Bootleg DDH6 (563.00–721.35 m depth), EHK Lisarow DDH1 (623.70–701.85 m depth), and DM Murray's Run DDH1 (739.85–783.94 m depth). Divisions between freshwater, brackish, and marine environments are based on the Sr vs Ba salinity proxy developed by Wei and Algeo (2020).

fluvial systems (Ashworth et al., 2015; Gugliotta et al., 2016). The abundant preservation of in situ glossopterid and other arborescent gymnosperm stumps and logs in both Facies B2 and B3 indicates that floodbasin environments were profusely vegetated at times, both in fresh and brackish water settings. Upright, in situ trees in places formed obstacles to water and sediment flow in crevasse sub-delta systems, as evidenced by tree stumps extending through erosionally-based, minor channel deposits (Fig. 4D). Matted concentrations of glossopterid leaves are interpreted to record seasonal (autumnal) leaf fall and accumulation on sediment surfaces in floodbasins. Facies B4 records periods of freshwater flooding of overbank environments either in the absence of, or distal to, sources of coarse-grained sediment. Such coastal plain lakes were likely shallow (< 2 m deep in most cases, judging by the thicknesses of overlying coarsening-upward cycles). Such shallow lake deposits host the rich fossil insect and branchiopod assemblages of the Belmont district south of Newcastle (Le Knight, 1950; Beattie, 2007).

4.1.3. *Facies Association C (FAC) – mire deposits*

Description. FAC comprises two facies, both of which entail accumulations of plant-derived organic matter as coal and coaly shale (Fig. 6A–D). Facies C1 accounts for discrete beds of coal up to several metres thick with subordinate clastic and volcaniclastic (Facies Association D) partings (e.g., Fig. 5A). Coal beds are laterally persistent across the region, but split and rejoin in either a simple dichotomous manner or, in some cases, in more complex styles. Coal seam splits are, in many cases, occupied by thick, lensoid, conglomerate and sandstone bodies of Facies A1. Coals are compositionally banded, and commonly preserve discrete lenses of bright coal (vitrinite) up to 0.1 m thick (e.g., Fig. 5C). Roots, typically referrable to *Vertebraria*, are common in clastic and volcaniclastic partings (e.g., Fig. 5B; Supplementary Fig. 2B). Upright, in situ tree stumps occur in the immediate roof of coal seams at several localities (e.g., Fig. 5D; Supplementary Fig. 2D). Plant fossil fragments overwhelmingly dominate the palynofacies assemblages for Facies C1 (81–98 %); one of these assemblages (S028841) has abundant charcoalified remains (Fig. 7G, H). Miospores (plant spores + pollen) form only a minor component (0.7–4.9 %), and algae (and probable algal acritarchs) are almost entirely absent (<0.1 %). Terrestrial organic microfossil concentrations for Facies B2 are exceptionally high (~2.7×10^6–$4.1 \times 10^6 \pm 18.7$–21.6 % fossils/g).

Facies C2 comprises intervals of thinly interbedded mudrocks, coal, coaly shale (impure coal), and minor sandstone (e.g., Fig. 5A, B). Such lithologies occur in various settings, but are particularly common immediately below coal seams of Facies C1. Complex roots systems of glossopterid trees are common, as are smaller root casts and coalified compressions referable to *Vertebraria*. Soft-sediment deformation is abundantly preserved in this facies, as are sedimentary breccias

comprising accumulations of plant fragments in a poorly sorted siltstone matrix. The palynofacies assemblages of Facies C1 and C2 are similar, but Facies C2 has higher proportions of amorphous organic matter (AOM; 15–45 %) and miospores (plant spores + pollen, 6.8–8.2 %), with correspondingly lower relative abundances of plant leaf and wood debris (48–77 %). Algae and acritarchs are very rare in Facies C2 (<1 %); almost all of those recovered were smooth-walled (*Leiosphaeridia* sp.) or spiny (e.g., *Micrhystridium*, Fig. 5B, C) acritarchs. Terrestrial organic microfossil concentrations for Facies C2 are very high (c. 1.2×10^6–$4.7 \times 10^6 \pm 16.9$–17.6 % fossils/g).

Interpretation. FAC is interpreted as the deposits of peat-forming mires, or coastal plain wetlands, such as are common in many present-day, low-lying, high-latitude terrains including the two largest sinks of terrestrial carbon on the planet (the West Siberian Plain and the Hudson Bay Lowland; Kremenetski et al., 2003; Martini, 2006). Facies C1 records accumulation of plant-derived organic matter in the virtual absence of dilution by clastic material, whereas Facies C2 likely represents mires where there was intermittent influx of clastic sediment, allowing for the interbedded character of this facies. The common association of in situ tree fossils with FAC suggests that formative mires were forested (i.e., swamps), and they were likely dominated by glossopterids. Although homogenization of plant tissues during coalification prevents definitive identification of plants in the coals, siliceous permineralized peat from coeval deposits of the western and southern parts of the basin (Pigg and McLoughlin, 1997; McLoughlin et al., 2019) confirm that such organic accumulations are overwhelmingly dominated by the remains of glossopterid gymnosperms—especially axial wood, roots and leaves. The presence of in situ stumps at the top of seams and palaeosols rich in *Vertebraria* beneath seams suggest that the bulk of the peat (coal) accumulated from autochthonous or parautochthonous plant remains. The combination of in situ stumps, roots, and woody and leafy palynodebris in Facies C1 are indicative of autochthonous deposits; this is in contrast with the parautochthonous palynofacies signature of Facies C2, which had more diverse assemblages, including algae, AOM and abundant dispersed plant propagules (spores and pollen). The consistent occurrence of spiny acritarchs—typically associated with marine deposits (Stancliffe and Sarjeant, 1994; Mays et al., 2021)—implicate marginal marine settings during clastic influx phases.

Again, given analogies with modern peat-forming mires (Dai et al., 2020), it is likely that peat accumulated at variable rates with hiatal periods recorded both by intra-coal seam surfaces and by clastic partings. The compositionally banded nature of coals suggests that water tables fluctuated frequently, giving rise to varying levels of oxidation of plant biomass (Suarez-Ruiz et al., 2012; Dai et al., 2020). Relatively high abundances of particulate amorphous organic matter (AOM) in Facies C2 is suggestive of the accumulation of microbial remains in intermittently stagnant, poorly oxygenated water (Tyson, 1995). Given the considerable thickness of some coals (up to 15 m), it is likely that peat accumulation was facilitated both by rapid rates of subsidence in the foredeep axial zone and by early compactional effects (cf. Van Asselen, 2011), in addition to rapid rates of biomass production. Net ecosystem productivity (sensu Lovett et al., 2006; Pace and Lovett, 2021) was relatively high in the high-palaeolatitude forests of the Sydney Basin based on growth rings in fossil woods that commonly reach a radial thickness of up to 10 mm. This is supported by the very high concentrations of plant remains in all palynofacies assemblages of Facies B2, C1 and C2, suggesting high levels of regional terrestrial productivity. This high productivity was achieved despite intermittent disturbance by wildfires (Fig. 5G, H), a phenomenon that has been recognized from other Permian wetlands of the Sydney Basin (Glasspool, 2000; Mays and McLoughlin, 2022). High biomass production is achievable at such latitudes, if the summer temperature and light regime is sufficient for rapid growth during the long spring–summer day lengths, and provided that temperatures were not excessively warm during winter darkness to cause energy loss through excessive respiration (Read and Francis, 1992).

4.1.4. Facies Association D (FAD) – pyroclastic fall and flow deposits

Description. FAD consists of one facies, D1 (Fig. 5E–H). The lithology is typically >95 % volcaniclastic material of silt to coarse sand grade, comprising a pale yellow to cream-coloured tuff. Several prominent tuff beds have been traced across the Newcastle Coalfield, and constitute important stratigraphic markers. Most variants of Facies D1 are stratified, in some cases diffusely and in others with clearly defined sedimentary structures. These include flat stratification, low-angle cross-bedding including backsets (e.g., Fig. 5G), high-angle cross-bedding, undulatory stratification, load casts and other soft-sediment deformation structures including large-scale convolute bedding. Intervals of Facies D1 range up to at least 30 m in thickness, and some are composite units with partings of other, terrigenous clastic deposits and coal (FAB and FAC; Fig. 5E, F). Coastal cliff exposures reveal a broadly tabular-bedded stacking pattern, with individual beds typically <1 m thick. Superimposed on this pattern are channel forms ranging up to tens of metres in width and < 8 m deep (Fig. 9). Some channel fills (e.g., Fig. 5F) are chaotic and include large, angular blocks of tuff in a coarse, tuffaceous matrix. Subsurface mapping by Creech (2007) indicated the preservation of linear, northeast-southwest-elongate belts of unusually thick (up to 30 m) tuff in four intervals up to 5 km wide. Maps of two tuffs (Nobbys and Awaba tuffs; Fig. 2) are presented in a modified form with additions from coastal exposures as Fig. 10.

A prominent feature of FAD is the preservation of in situ and detrital tree fossils and associated large woody debris (Supplementary Fig. 2C, E, F). Fossil trees are predominantly glossopterid but, based on associated leaf remains, other woody plants (cordaitaleans and voltzialean conifers) may also have been present in the local vegetation. These woody remains include upright, tilted, and flattened, in situ stumps attached to root systems (Supplementary Fig. 2C, D), some with associated centroclinal cross-bedding (Underwood and Lambert, 1974, e.g., Fig. 5H). At several localities (e.g., Reids Mistake, north end), tilt directions of inclined stumps coincide with the orientations of flattened plant axes and with azimuths of cross-bedding. Partially intact plant fossils with branches and roots are also found encased within tuff beds, in at least one case (Reids Mistake, below Coastguard Station) upside down. In some localities (e.g., Fig. 5E), FAD is repeatedly interbedded with coal and coaly shale beds of FAC.

Interpretation. The volcaniclastic composition of Facies D1 indicates that it was sourced from volcanic eruptions and shed into the foredeep of the retroarc foreland Sydney Basin. The tuffs retain remnant quartz, biotite, K-feldspar, and plagioclase crystals, together with lithic fragments, but are otherwise altered to kaolinite, mixed-layer illite/smectite clays, secondary calcite and siderite. This, together with geochemical (Zr/TiO_2 and Nb/Y) data for the upper Permian tuffs of the Sydney Basin, suggests derivation from rhyodacitic to dacitic sources of a continental volcanic-arc setting (Kramer et al., 2001; Grevenitz et al., 2003). Palaeocurrent directions from sedimentary structures and flattened plant axes indicate that the source volcanoes were located to the east, and palaeoflows were directed westward, at least in coastal exposures (David, 1907; Diessel, 1984, 1992, Fig. 7). Most Facies D1 beds are almost entirely composed of volcaniclastic debris (crystals, devitrified ash) with mixing of terrigenous clastic sediment in some cases. This suggests that the formation of tuffs was by processes distinct from "normal" depositional processes active in the basin, and points towards some combination of pyroclastic fallout, pyroclastic flow/surge, and local epiclastic reworking of volcanic debris. However, there is no evidence of welding in the tuffs, no preserved pumice fragments or "fiamme", such as are diagnostic of classical pyroclastic flow deposits (ignimbrites), and stratification is abundantly preserved, suggesting that formative flows may have been at more or less ambient temperatures. Furthermore, preserved plant fossils were flattened but not incinerated, given their mode of preservation.

The preservation of abundant upper flow regime structures suggests

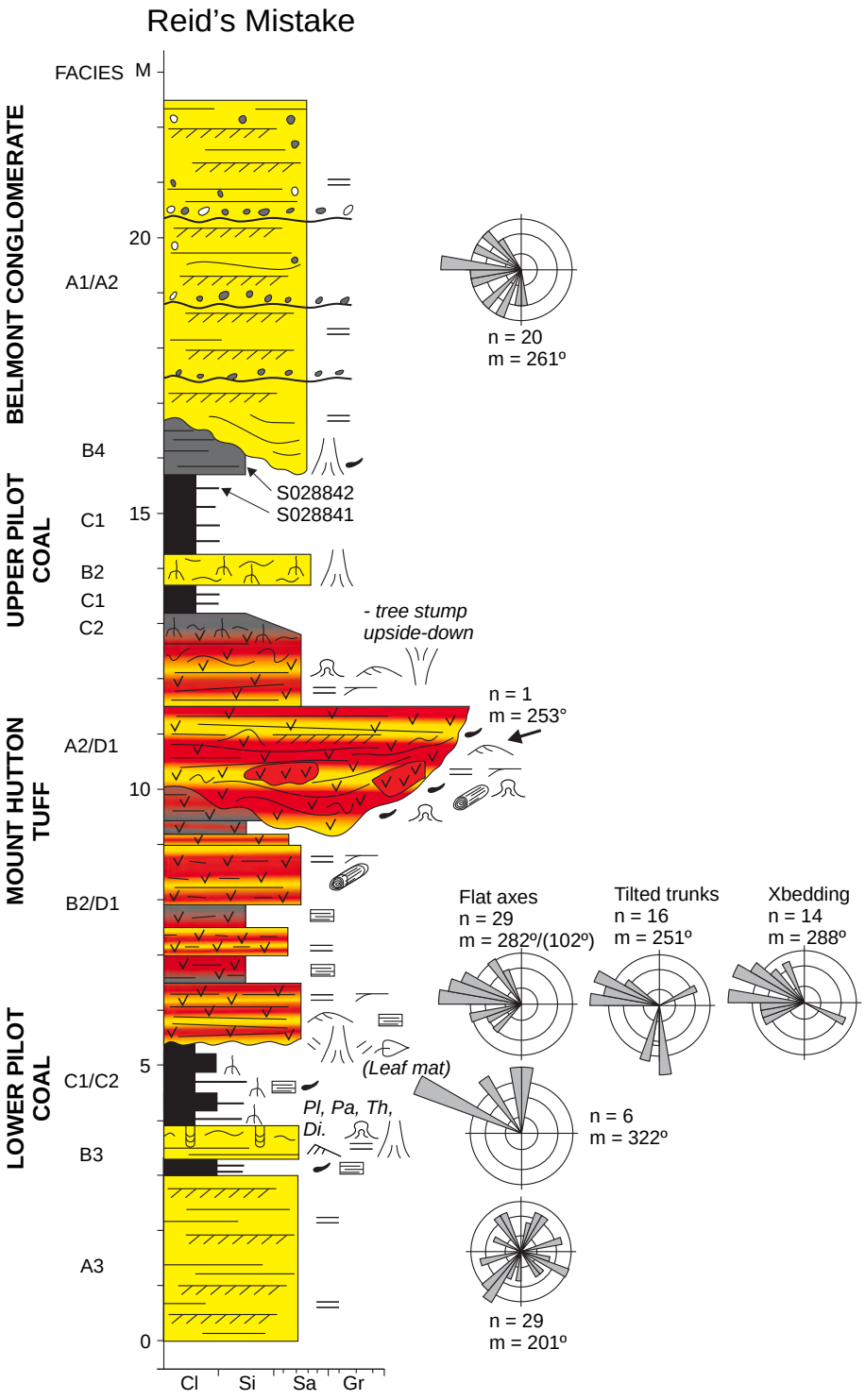

Fig. 9. Graphic log of the exposed section at the south end of Reids Mistake (near Illawong Park). The Lower and Upper Pilot Seams are separated by a major tuff interval (Mount Hutton Tuff) that preserves upright and tilted, in situ tree stumps, detrital plant axes, a variety of upper flow regime sedimentary structures, and at the south end of the outcrop belt a channel form filled chaotically with tuff and large tuff clasts (Fig. 5F). Above the Upper Pilot Seam is the erosionally-based Belmont Conglomerate (Facies A1) which preserves an upright, in situ fossil tree near its base (Fig. 3F).

that many formative flows were powerful and turbulent. Recognition of channel forms filled by Facies D1 suggests that formative flows were, at least in part, confined to channels incised into precursor deposits and into pyroclastic deposits (e.g., Figs. 5F, 9). The chaotic nature of some channel fills (including "floating" angular boulders of tuff) and diffuse or absent stratification suggests that some of those formative flows were poorly organized and transitional between turbulent and laminar, with high particle concentrations and elevated suspended mud contents (cf. Baas et al., 2016). These flows were, in some cases, sufficiently powerful to flatten trees in the direction of flow or to uproot and transport vegetation (also see Brakel et al., 1995) but, in others, moved around trees and encased them rapidly in volcaniclastic material, preserving either upright or tilted stumps surrounded by centroclinal cross-bedding (e.g., Fig. 5H). Such phenomena indicate rapid rates of sediment

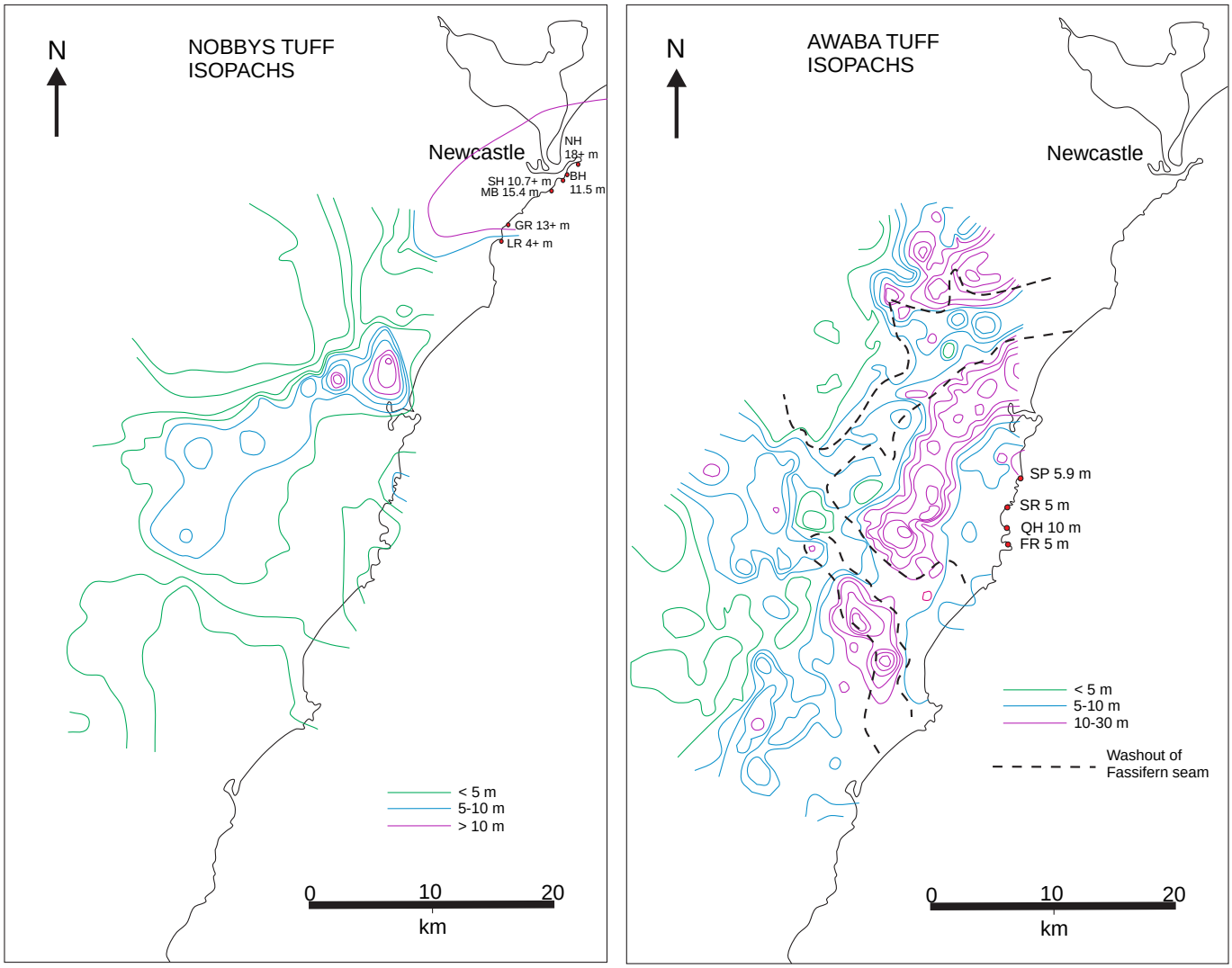

Fig. 10. Isopach maps of A) Nobby's Tuff and B) Awaba Tuff (Fig. 2), modified after maps by Creech (2007) and augmented with outcrop data from coastal exposures. Both maps show linear, southwest-trending belts of thick tuff up to 30 m thick and 5 km wide that turn southward to parallel the trends of channel bodies (Fig. 11). These are interpreted to record valley fills that either pre-existed and were exploited by pyroclastic flows, or were cut during the volcanic episodes represented by the tuffs. See Fig. 6 for palaeocurrent data from Nobbys Tuff, which indicate west- to southwestward flow consistent with isopach patterns.

accretion, possibly >1 m over timeframes of days to weeks. However, the thickness of some tuff intervals, presence of in situ, upright tree fossils within tuff intervals, and interbedding with FAC indicates that many tuffs are composite bodies that accumulated over extended periods of time that were characterized by multiple eruptive events (Fig. 5E). That there are several such tuff bodies preserved in the Newcastle Coal Measures indicates that the formation accumulated during a period of frequent, explosive volcanic eruptions in the volcanic arc to the east (Diessel, 1984; Bradley, 1993; Grevenitz et al., 2003; Chapman et al., 2022). Literature suggests that pyroclastic density flows on land from historical eruptions have typical runout distances of up to a few tens of km (e.g., Lajoie, 1984; Roche et al., 2021), suggesting that the Newcastle Coalfield exposures lay at the outer limit of this range from the formative volcanoes. Since the modern continental shelf off the northern Sydney Basin is 50–60 km wide, the source volcanoes were likely positioned in this region or on what is now the Dampier Ridge of the Lord Howe Rise, which hosts granitic rocks of Permian age (McDougall et al., 1994) and was adjoined to eastern Australia before the Cretaceous breakup of Zealandia and Australia (Willcox et al., 2001). The presence of linear belts of thick tuff at several stratigraphic intervals suggests that the powerful flows that deposited tuffs either cut valleys or occupied pre-existing valley topography (Fig. 10). The northeast-southwest orientation of many of these belts suggests that once they entered the foredeep of the Macquarie Syncline, they rotated to follow the southward regional palaeoslope (Fig. 10).

4.2. Biostratigraphy

All palynomorph assemblages examined herein are consistent with the *Dulhuntyispora parvithola* Zone (= APP5 zone). This zone is characterized by the distinctive fern spore *D. parvithola* (Fig. 7A; Foster, 1972) and the absence of APP6 index taxa (e.g., *Triplexisporites playfordii*; Mays et al., 2020; Amores et al., 2025). None of the spore or pollen taxa (e.g., *Dulhuntyispora inornata*, *D. stellata*, *Microreticulatisporites bitriangularis*) utilized by Price (1983, 1997) to subdivide the *Dulhuntyispora parvithola* Zone in the contiguous the Bowen Basin was found. The short-spined acritarch *Micrhystridium evansii* was present (Fig. 7B), but not in the high abundances typical of the *M. evansii* Abundance (=Acme) Zone. This abundance zone has been recorded within the Denison Trough, Springsure Shelf, and Comet Platform of the Bowen Basin (Evans, 1962; Price, 1983; McLoughlin, 1990; Fielding et al., 2022), but not yet from the Sydney Basin. Although its presence supports mixohaline

depositional conditions (Fielding et al., 2022), this taxon has been recorded below and above the *M. evansii* Abundance Zone (Price, 1997). For these reasons, the targeted localities could not be constrained biostratigraphically beyond the broad *Dulhuntyispora parvithola* Zone [Lopingian].

5. Discussion

5.1. Alluvial architecture

The cross-sectional stratal architecture of the Newcastle Coal Measures has been investigated by numerous prior workers, who have collectively established that coarse-grained (Facies Association A, FAA) alluvial channel bodies are elongate in a broadly north-south direction and lensoid east-west (e.g., Branagan & Johnson, 1970; Warbrooke, 1984; Bocking et al., 1988; Diessel, 1992; Boyd et al., 1998; Lindsay and Herbert, 2002; Fielding et al., 2021; Fig. 11). The observation by all these authors that the lateral pinchout margins of many FAA bodies merge into coal seam splits indicates that channel activity was broadly contemporaneous with peat accumulation at the coalfield scale (e.g., Figs. 12, 13). Examples of both offset (compensational) stacking, indicating an autogenic (probably compactional) control on channel location, and vertical stacking, indicating a structural control, have been noted by previous workers. Bocking et al. (1988) documented a series of offset (compensationally) stacked channel bodies in the southern part of the Newcastle coalfield, in a direction perpendicular to the dispersal direction (their Fig. 2). Branagan & Johnson (1970, p. 26) noted a series of vertically stacked channel bodies in parts of the coalfield, coincident with the trace of known faults, and suggested a tectonic control on stacking patterns. We observed one set of four successive FAA bodies in the upper NCM repeatedly following much the same track, with some offset between one body and the next (Fig. 10). This suggests that the over-riding control on channel belt location and orientation was the location and trend of the foredeep axis.

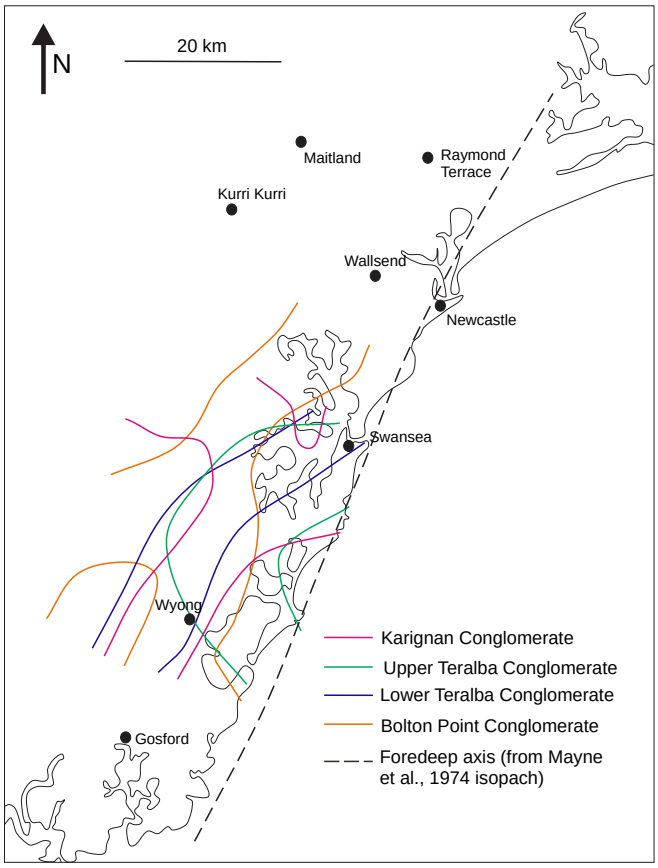

Fig. 11. Map of the Newcastle Coalfield showing the extents and orientations of channel belt deposits (Facies Association A) in the upper Newcastle Coal Measures, mapped by Bocking et al. (1988) and Fielding et al. (2021). Four successive conglomerate bodies are shown: 1. Bolton Point Conglomerate, 2. Lower Teralba Conglomerate, 3. Upper Teralba Conglomerate, and 4. Karignan Conglomerate (see Fig. 2 for stratigraphy, and Figs. 12 and 13 for cross-sectional illustrations). Also shown is the trend of the foredeep axis as interpreted from the Newcastle Coal Measures isopach map of Mayne et al. (1974).

Many FAA bodies are completely enclosed by coal seam splits (e.g., Figs. 12, 13), indicating that they represent alluvial channel belts of limited lifespan that formed within areas formerly occupied by peat-forming mires. Examples of both convergent (tributive; e.g., Branagan & Johnson, 1970, fig. 31 and Fielding et al., 2021, Fig. 5C,) and divergent (distributary or avulsive; Branagan & Johnson, 1970, fig. 28) patterns have been illustrated by those who have attempted to map channel bodies (and see also Fig. 11). Mapped trends are consistent with palaeoflow directions as determined from sedimentary structures in locations where these bodies crop out at the surface (e.g., Fielding et al., 2021, Fig. 5).

Previous workers have examined whether channels were active simultaneously with peat accumulation, or formed and filled in separate episodes (e.g., Diessel, 1992; Lindsay and Herbert, 2002). One model popular among researchers entails the progressive collapse of peat bodies under the weight of contemporaneous, gravelly channel sediment in a direction perpendicular to flow (and thus, to channel body elongation direction). In this way, the macroform dipping surfaces that are a feature of FAA bodies formed via progressive tilting of bedding surfaces towards the site of peat compaction (Diessel, 1992, Fig. 6.50). There is, however, no known modern analogue for such a process (see also Fielding and Alexander, 2001). Furthermore, this model also invokes sediment dispersal on braidplains, where from modern examples it is clear that channels are highly mobile and “comb” the channel belt in multiple directions rather than in one, consistent direction. It is also evident that the macroform dipping bedding surfaces are in fact lateral accretion sets formed on the inner banks of sinuous river channels (see above).

An alternative model (Lindsay and Herbert, 2002) entails the incision and infilling of valleys during hiatuses in peat accumulation, controlled by relative sea-level change. A corollary of this model is that channel body bases represent sequence boundaries in the genetic sense. The fatal problem with this interpretation is that there is very little evidence for erosional relief on the bases of FAA bodies (e.g., Figs. 12, 13); rather, they conformably overlie coal seams or “roof” strata in almost all cases, with only local evidence of modest (<5 m) erosional excision. There is no evidence for 10s of metres of erosional relief at the base of FAA bodies anywhere in the Newcastle coalfield. Further, since many FAA bodies are enclosed on both lateral margins by coal bodies, their basal surfaces pass directly into those coal bodies where they display no evidence of exposure or relative base-level lowering. This argument is made in considerable detail by Little & Boyd (in Boyd et al., 1998). Nonetheless, elements of the Lindsay and Herbert (2002) model seem valid, among them that formation and filling of channels probably occurred during hiatuses in peat accumulation. Many FAA intervals are multistorey bodies and so are at the geomorphic scale of valley fills, but they are not significantly incised. Early (near-surface) peat compaction almost certainly played a role in creating the accommodation necessary to preserve conglomerate and sandstone bodies up to tens of metres thick.

5.2. Stratigraphic trends

Perceived gradual upward changes in the distribution and proportion of facies (Engel, 1966; Herbert, 1980; Warbrooke, 1987; Diessel, 1989; Hawley and Brunton, 1995) and in the organic petrology of coals (Diessel, 1986, 1992; Warbrooke, 1987) led those authors to postulate a

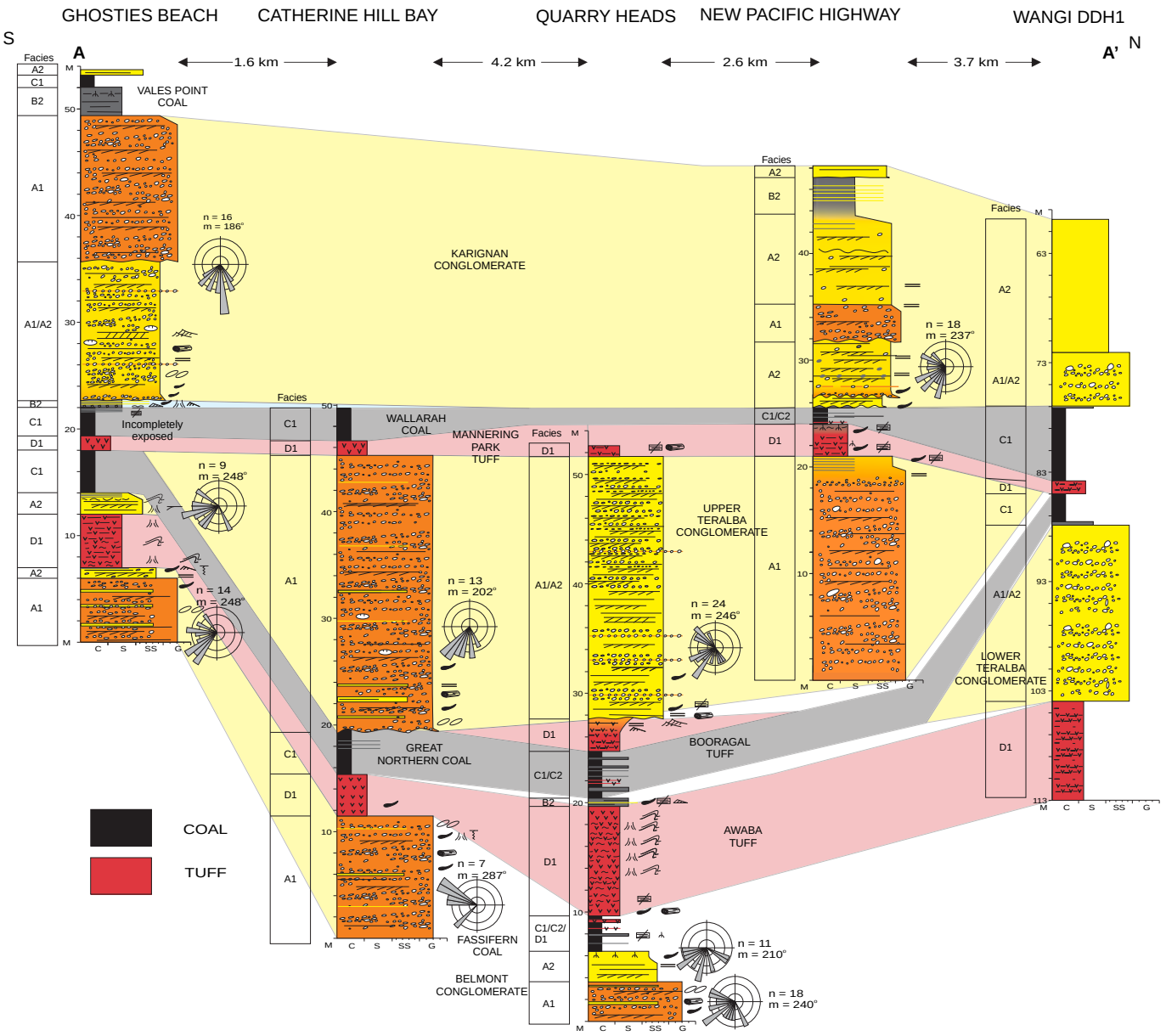

Fig. 12. North-south cross-section from DM Wangi DDH1 to surface exposures at Ghosties Beach illustrating the lensoid cross-sectional geometry of the Upper Teralba Conglomerate which is enclosed by a coal seam split between the combined Great Northern and Wallarah Seams in the north and south. The correlations are further strengthened by the recognition of the Awaba, Booragul, and Mannering Park tuffs in this uppermost part of the Newcastle Coal Measures. See Fig. 1 for locations.

progressive upward change in depositional environment from lower delta plain, through upper delta plain, to fluvial braidplain with base-of-slope alluvial fans, from base to top of the Newcastle Coal Measures. This theme was taken up by Breckenridge et al. (2019) and Melehan et al. (2021), who postulated a basin-wide, erosional disconformity separating the delta plain from the overlying fluvial interval. However, the "surface" they illustrated (fig. 19 of Breckenridge et al., 2019) is, in reality, at least three separate surfaces (base of Merewether Conglomerate from King Edward Park to Merewether, base of Redhead Conglomerate at Redhead (Fig. 6), and base of Belmont Conglomerate at Swansea and Caves Beach (Fig. 9), and thus is illusory.

Breckenridge et al. (2019) further asserted that their erosionally based fluvial succession overlies a major sequence boundary and records the topset of a lowstand systems tract genetically unrelated to underlying strata. However, since their single erosion surface does not exist, there is no reason for this to be the case. All attempts to map coarse-grained channel bodies in the Newcastle Coal Measures (e.g., Bocking et al., 1988; Agnew et al., 1995; Lindsay and Herbert, 2002; Fielding et al., 2021) have concluded that they define linear belts <20 km wide (Fig. 11), enclosed laterally by coal seam splits (e.g., Fig. 12) and, therefore, have no regional, genetic stratigraphic significance. They are, furthermore, distributed throughout the NCM from base to top (Fig. 2), and the facies assemblage is invariant throughout the NCM.

Our investigations conclude that although there is a subtle (and irregular) upward increase in sediment caliber, and a similarly subtle upward decrease in evidence of tidal processes, the overall depositional setting of the Newcastle Coal Measures remains similar throughout. Whereas some authors (Herbert, 1997; Breckenridge et al., 2019) have sought to apply sequence stratigraphic coding to this succession, most evaluations have concluded that the Newcastle Coal Measures cannot be rationalized in sequence stratigraphic terms (e.g., Little, 1998; Boyd et al., 1998). This is because it is impossible to rigorously identify

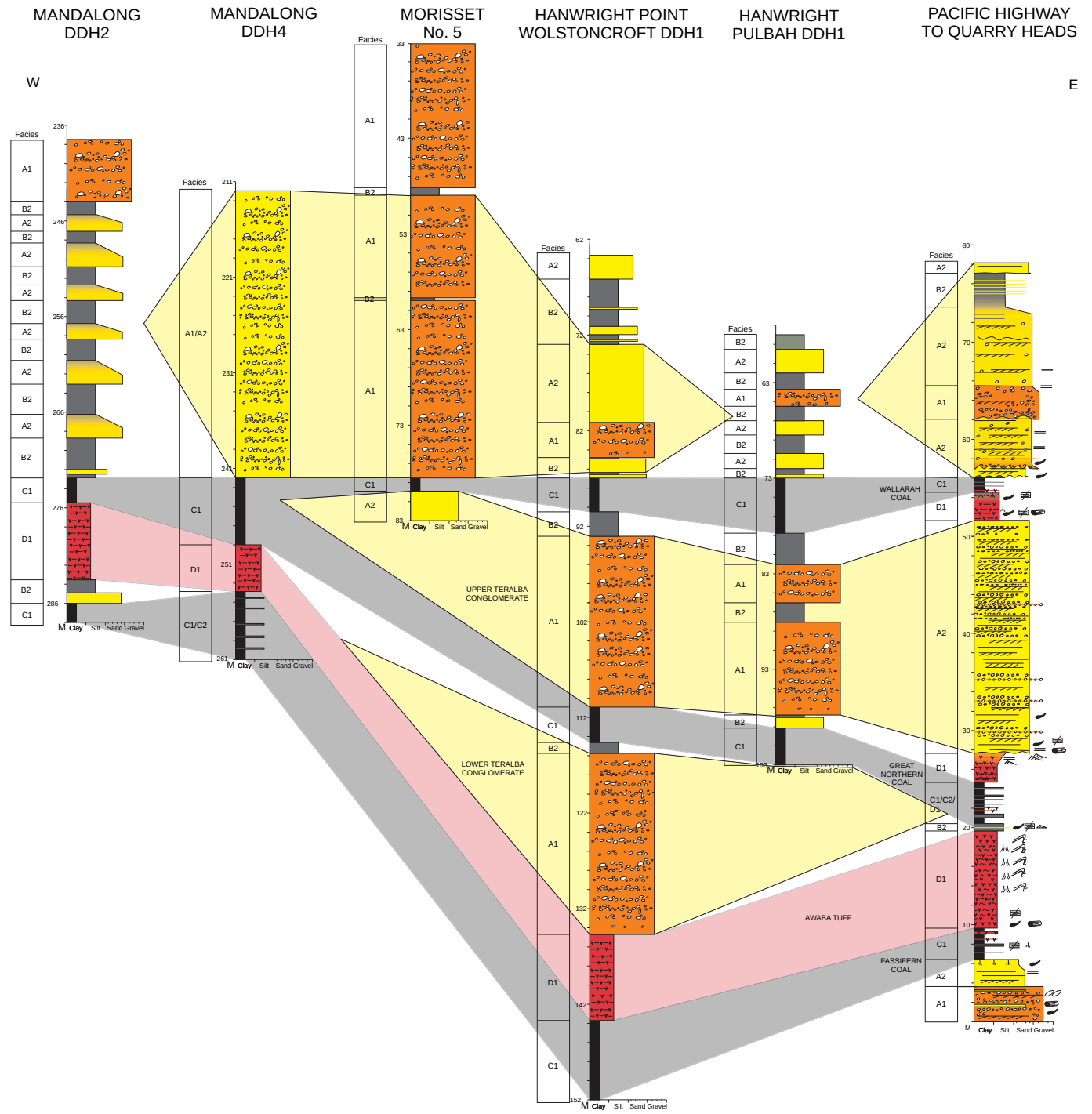

Fig. 13. West-east cross-section from DM Mandalong DDH2 to coastal exposures in the vicinity of Quarry Heads, showing the lensoid cross-sectional geometry of three FAA bodies in a direction perpendicular to palaeoslope. Again, correlations are assisted by the preservation of distinctive tuff and coal beds. See Fig. 1 for locations.

regionally traceable erosion surfaces (sequence boundaries), flooding surfaces, or maximum flooding surfaces (since there are no regional flooding events recorded in the Changhsingian). It is likely that this is owed in large part to the rapid rates of accommodation and of coarse sediment supply into the basin, which suppressed relative sea-level drawdowns and rises, respectively.

5.3. Sediment dispersal patterns and palaeogeography

An overall southward sediment dispersal pattern is indicated for the Newcastle Coal Measures, both from maps of channel belts and from palaeocurrent data sets. Data both from this study and from previous publications indicate that these patterns apply to the entire unit. A previous interpretation of Facies A1 conglomerates as deposits of westward-sloping alluvial fans (Blayden, 1984) is not supported either by palaeocurrent data or by the confinement of Facies A1 to linear, southward-trending belts (Fig. 11). That said, there is evidence for westward-directed sediment transport in FAD (volcaniclastic deposits). This suggests that a topographic basin margin lay a few tens of km to the east from the Newcastle Coalfield and that the adjacent orogen

experienced repeated volcanic activity, leading to the dispersal of volcaniclastic debris into the basin from the east (see also Bradley, 1993). Palaeocurrent data from earliest Triassic strata begin to show evidence of westward dispersal, suggesting that, by this time, orogenic mountain front fans had prograded sufficiently far westward to impinge upon the Newcastle area (Fielding et al., 2021 Fig. 5D).

Almost all published palaeogeographic maps of the northern Sydney Basin show the present, northern and northeastern structural margin as coincident with the original topographic basin margin (e.g., Herbert, 1980, 1997; Jones et al., 1987; Cowan, 1993), and assume that the northwest-southeast trend of the present-day Sydney Basin synclinal axis coincides with its original trend. The northeast boundary is, nonetheless, structurally complex and in many places overthrusted (the Hunter-Mooki Thrust System). Neither its location nor its orientation need, therefore, show any relationship to the original basin boundary. There is no fringing apron of upper Permian, coarse-grained deposits around this margin that might speak to its role as a topographic boundary, despite such features being shown on some palaeogeographic maps (e.g., Herbert, 1980). Furthermore, isopachs of both the Newcastle Coal Measures and the underlying Tomago Coal Measures (Mayne et al., 1974) trend north–south to north-northeast–south-southwest and intersect the structural basin boundary at a high angle. Stratigraphic equivalents of upper Permian and Triassic units are also preserved in synclinal axes (Gloucester and Myall Synclines, Cranky Corner Basin) and outliers (Lorne Basin), respectively, to the north of this boundary. All this suggests that the original extent of the Sydney Basin has been significantly modified by contractional deformation associated with the Hunter-Bowen Event (Holcombe et al., 1997; Glen, 2005; Rosenbaum, 2018) and that the basin originally extended considerably northward of the Hunter-Mooki Thrust.

A more parsimonious palaeogeography for the northern Sydney Basin entails a north-south-elongate geometry extending northward into what is now the southern New England Foldbelt, considerably wider than the preserved structural limit of the basin (Figs. 14, 15). In this scenario, formation of the onshore New England Foldbelt, which caused significant narrowing of the preserved basin, had not yet begun by the late Permian. This modified palaeogeography provides a more logical explanation for the broad, southward-draining (basin-axial) channel belts preserved in the Newcastle Coal Measures. This is because the substantial FAA conglomerate and sandstone bodies likely represent trunk rivers of considerable dimensions that would have had long courses. Lengthy, well-established fluvial drainage networks are also implied by the rounded to well-rounded modal shape of gravel in Newcastle Coal Measures conglomerates (Fig. 3), which could only have been achieved after a considerable distance of surface transportation (or by reworking from older deposits). Supply of gravel into the foredeep was evidently pulsed, and may reflect cycles of thrust propagation and construction of orogenic topography. Climatic cycles may also have contributed to the apparently episodic delivery of coarse sediment, allowing extended periods for thick peat bodies to accumulate in the rapidly-subsiding foredeep trough.

Although a dominance of southward sediment dispersal is indicated for the upper Permian, the Lower Triassic (Narrabeen Group) succession shows increasing influence of westward-directed sediment dispersal (Ward, 1972; Goldbery and Holland, 1973; Bradley, 1993), along with continuation of southward, axial drainage (Fielding et al., 2021). East-directed sediment dispersal is also indicated, particularly from sites on the western margin of the basin (Goldbery and Holland, 1973), and Cowan (1993) presented palaeocurrent data from coastal exposures that he suggested also indicate eastward dispersal in some intervals. Petrographic data indicate that much of the westward-dispersed sediment had a first-cycle volcanic provenance (Ward, 1972), and was likely derived from the emerging continental volcanic arc that is now submerged offshore (Bradley, 1993), whereas other sediment was derived from cratonic sources (Ward, 1972; Cowan, 1993).

A general southward decrease in the abundance of conglomerates has been noted in the Newcastle Coal Measures and equivalents. Southward from the Newcastle coalfield into the present-day synclinal axis (under Sydney) and further south to the Illawarra region, the equivalent stratigraphy also preserves increasing, fine-grained, paralic or fully marine transgressive-regressive wedges, such as the Wilton Formation and Bargo Claystone (Bamberry et al., 1995). But these fine-grained intervals are enclosed vertically by sandstone-rich, coastal alluvial plain facies similar to the Newcastle Coal Measures. These patterns suggest that, whereas the central and southern Sydney Basin were closer to a marine inlet (perhaps a gulf located still further south), those areas were not fully marine during the late Permian as depicted by Herbert (1980), his Figs. 2.16 and 2.17).

The closest modern analogue to the late Permian Sydney Basin is the western Kamchatka Peninsula, Russia, and adjacent Sea of Okhotsk, which are broadly north-south-elongate, located in high latitudes, and host extensive peatlands subjected to regular blankets of tephra from explosive volcanic eruptions (Zakharikhina, 2014). The northeastern Sea of Okhotsk closes in a narrow embayment fed by rivers (including

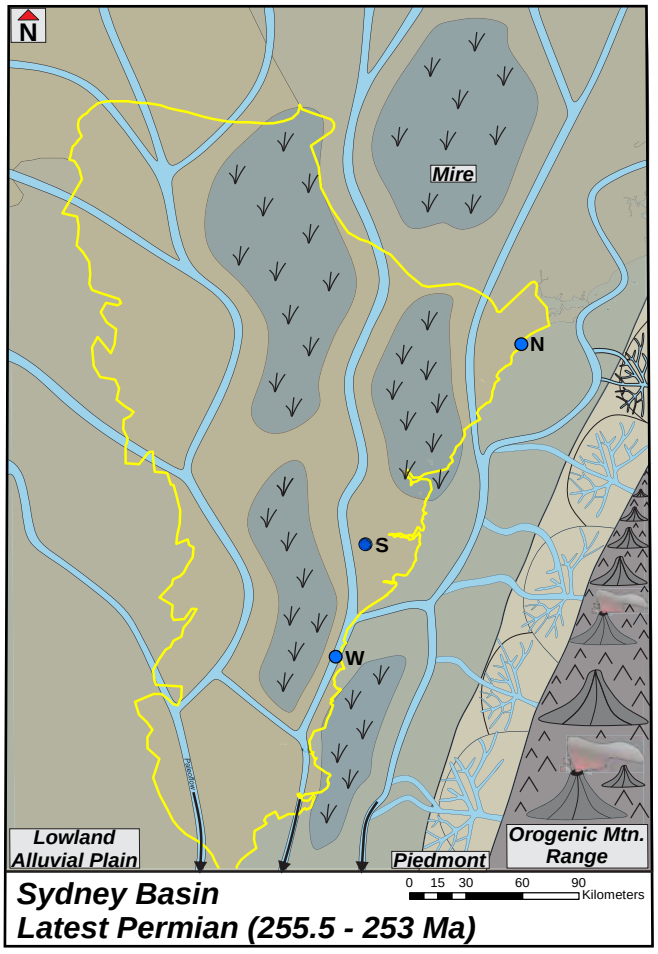

Fig. 14. Palaeogeographic reconstruction of the Sydney Basin during accumulation of the Newcastle Coal Measures and equivalents. The map is constructed to extend the basin north of the Hunter-Mooki Thrust, since evidence indicates that structural shortening associated with the Hunter-Bowen Event had not yet reached this part of the foreland (see text for further detail). The map portrays dominantly southward (basin-axial) sediment dispersal across a coastal alluvial plain, with some sediment shed from a rising orogenic hinterland to the east, and intermittent supply of volcaniclastic debris from eruption of stratovolcanoes located in that mountain range. Modern onshore extent of the Sydney Basin outlined in yellow. Modified from Fielding et al. (2021). N – Newcastle, S – Sydney, W – Wollongong. (For interpretation of the references to colour in this figure legend, the reader is referred to the web version of this article.)

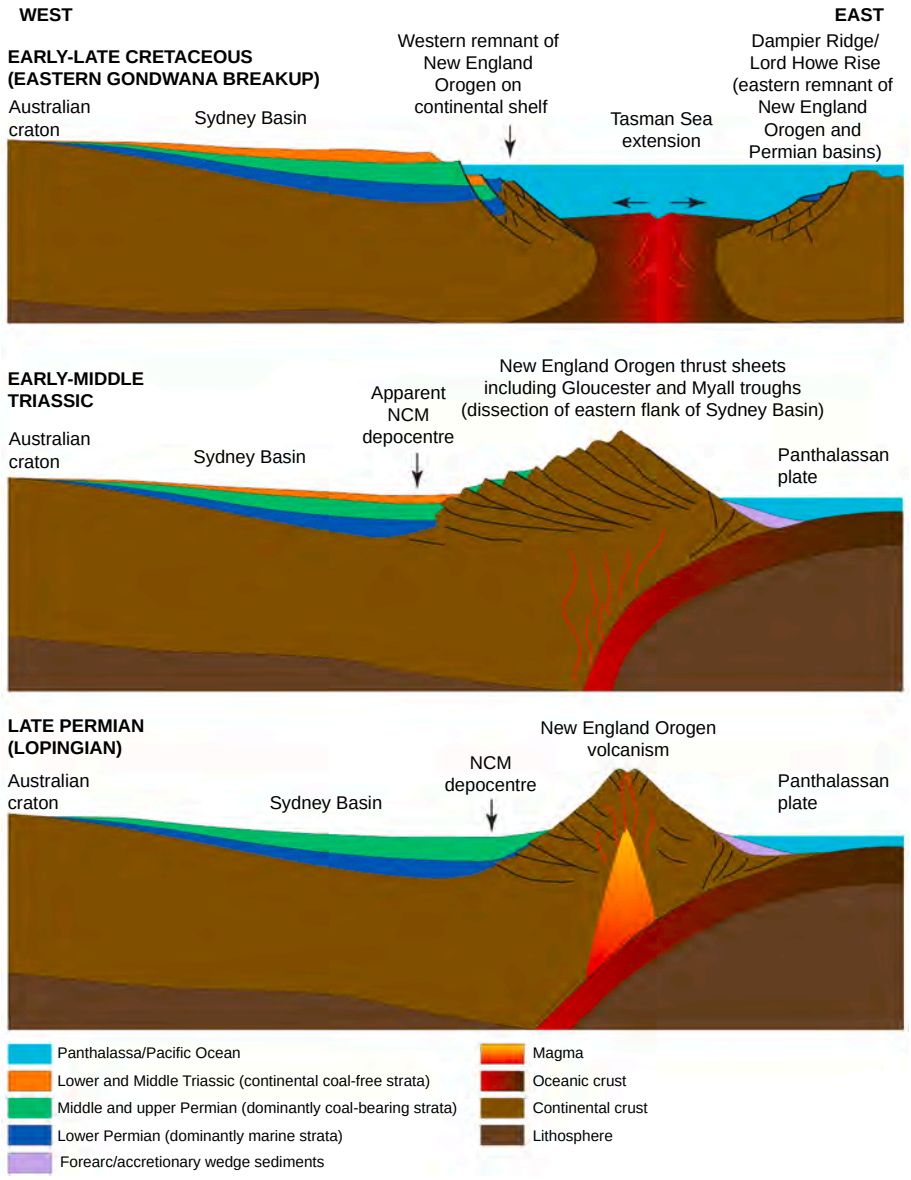

Fig. 15. A series of schematic cross-sections from onshore New South Wales (west - left) to offshore (east - right), illustrating the interpreted tectonic context of the retroarc foreland Sydney Basin from deposition of the Newcastle Coal Measures (Lopingian), through its closure during the Triassic to its later partial dismemberment during Cretaceous rifting. The lowest panel shows the periodically volcanically active setting for the NCM, which was also likely affected at times by thrust sheet propagation to form a foredeep trough.

the large, megatidal Penzhina River) draining both continental volcanic arc terrains (to the east) and cratonic terrains (to the west). Regrettably, there is virtually no literature on the surface geomorphology or subsurface stratigraphy of this region from which to draw detailed comparison.

6. Conclusions

The upper Permian Newcastle Coal Measures formed in a coastal alluvial plain environment, in the foredeep axis of a retroarc foreland basin. Four facies associations are interpreted as the deposits of major alluvial channel belts, floodplains and floodbasins, mires, and emplacement of volcaniclastic debris from contemporaneous eruptions along a convergent-margin arc to the east, respectively. Coarse-grained channel bodies describe north-northeast–south-southwest-trending belts up to 20 km wide and are tens of metres thick. The consistent directional trend and overlapping positions of successive channel belt bodies are interpreted to reflect a combination of compensational stacking of incompactible gravel and sand-grade bodies, together with the overriding control of the foredeep axis, which maximized accommodation. The controlling role of the foredeep is also illustrated by isopachs of prominent volcaniclastic beds, which also show south-southwest-trending thick belts interpreted as recording excision and/or filling of valley topography parallel to the foredeep axis. The preservation of thick alluvial conglomerate bodies in the section is anomalous in the context of alluvial coal-bearing successions worldwide, particularly for regions with such high primary productivity. But this unusual combination of thick alluvial coal and conglomerate bodies is explained by the high accommodation rate in the foredeep axis (estimated at 15 cm/1000 yrs. uncompacted, or 34 cm/1000 yrs. allowing for compaction), together with proximity to a rising orogenic highland that supplied coarse-grained sediment to the basin.

Despite being within the backwater zone and, therefore, subject to tidal influences, the Newcastle Coal Measures show no preservation of coherent, genetic sequence architecture forced by relative sea-level fluctuations. No regionally traceable erosion surfaces that might

represent sequence boundaries are present, nor are widespread flooding surfaces preserved. The lack of recognizable sequence boundaries is attributed to the high accommodation regime, likely assisted by early compaction of thick peat bodies in the near-surface realm; and the lack of preserved flooding surfaces can be attributed to high rates of coarse sediment supply, which maintained the coastal alluvial surface throughout the ~3 m.y. interval over which the Newcastle Coal Measures accumulated. Stable relative sea-levels and an absence of major biostratigraphic events were promoted by a generally consistent humid temperate climate. Overall, the Newcastle Coal Measures accumulated under the overwhelming control of tectonic and early compactional accommodation, with minimal influence of relative sea-level change. It forms an example of a conglomerate-bearing coal measure succession that did not significantly involve base-of-slope fans at a basin margin.

Supplementary data to this article can be found online at https://doi.org/10.1016/j.coal.2025.104829.

CRediT authorship contribution statement

Christopher R. Fielding: Writing – original draft, Supervision, Methodology, Investigation, Conceptualization. **Stephen McLoughlin:** Writing – review & editing, Investigation, Funding acquisition, Data curation. **Chris Mays:** Writing – review & editing, Investigation, Funding acquisition, Data curation. **Allen P. Tevyaw:** Visualization, Investigation. **Tracy D. Frank:** Writing – review & editing, Investigation, Formal analysis.

Declaration of competing interest

The authors declare the following financial interests/personal relationships which may be considered as potential competing interests:

Steven McLoughlin reports financial support was provided by Swedish Research Council. Chris Mays reports financial support was provided by Irish Centre for Research in Applied Geosciences. Chris Mays reports financial support was provided by Frontiers for the Future Programme (Science Foundation Ireland). If there are other authors, they declare that they have no known competing financial interests or personal relationships that could have appeared to influence the work reported in this paper.

Acknowledgements

Editor S.F. Dai, referees A. Amorosi, A. Maravelis, and two anonymous individuals are thanked for their comments on the submitted manuscript. S. McLoughlin was funded by a Swedish Research Council (Vetenskapsrådet) grant (2022-03920). C. Mays was supported by the Irish Centre for Research in Applied Geoscience (Science Foundation Ireland), Grant number #13/RC/2092_P2 and by the Frontiers for the Future Programme (Science Foundation Ireland), Grant number #22/FFP-P/11448. We thank the staff at the W.B. Clarke Geoscience Centre in Londonderry, Sydney (New South Wales) for facilitating access to drillcores used in this study.

Data availability

All data used in this research/paper are presented in Figures, Tables, or in Supplementary files.

References

Agnew, D., Bocking, M., Brown, K., Ives, M., Johnson, D., Howes, M., Preston, B., Rigby, R., Warbrooke, P., Weber, C.R., 1995. Sydney Basin – Newcastle Coalfield. In: Ward, C.R., Harrington, H.J., Mallett, C.W., Beeston, J.W. (Eds.), Geology of Australian Coal Basins, Geological Society of Australia Coal Geology Group Special Publication, vol. 1, pp. 197–212.

Aitken, J.F., Flint, S.S., 1995. The application of high resolution sequence stratigraphy to fluvial systems: a case study from the Upper Carboniferous Breathitt Group, eastern Kentucky, USA. Sedimentology 42, 3–30. https://doi.org/10.1111/j.1365-3091.1995.tb01268.x.

Allen, P.A., Allen, J.R., 2013. Basin Analysis: Principles and Application to Petroleum Play Assessment (3rd Edition). Wiley-Blackwell, Oxford, 619 pp.

Amores, M., Frank, T.D., Fielding, C.R., Hren, M.T., Mays, C., 2025. Age-controlled south polar floral trends show a staggered Early Triassic gymnosperm recovery following the end-Permian event. GSA Bull. https://doi.org/10.1130/B38017.1.

Ashworth, P.J., Best, J.L., Parsons, D.R. (Eds.), 2015. Fluvial-Tidal Sedimentology. Developments in Sedimentology, vol. 68. Elsevier Science, Amsterdam, 719 pp.

Baas, J.H., Best, J.L., Peakall, J., 2016. Predicting bedforms and primary current stratification in cohesive mixtures of mud and sand. J. Geol. Soc. Lond. 173, 12–45. https://doi.org/10.1144/jgs2015-024.

Balme, B.E., Hennelly, J.P.F., 1956a. Trilete sporomorphs from Australian Permian sediments. Aust. J. Bot. 4, 240–260. https://doi.org/10.1071/BT9560240.

Balme, B.E., Hennelly, J.P.F., 1956b. Monolete, monocolpate, and alete sporomorphs from Australian Permian sediments. Aust. J. Bot. 4, 54–67. https://doi.org/10.1071/BT9560054.

Bamberry, W.J., Herbert, C., 1996. Fluvial Successions of the Late Permian to Triassic rocks of the northern Sydney Basin. Australasian Association of Sedimentologists Field Guide Series. Geological Society of Australia, Springwood, NSW, Australia, p. 64.

Bamberry, W.J., Hutton, A.J., Jones, B.G., 1995. The Permian Illawarra Coal Measures, southern Sydney Basin, Australia: A case study of deltaic sedimentation. In: Postma, G., Oti, M.N. (Eds.), Geology of Deltas. A.A. Balkema, Rotterdam, pp. 153–166.

Beattie, R., 2007. The geological setting and palaeoenvironmental and palaeoecological reconstructions of the Upper Permian insect beds at Belmont, New South Wales, Australia. Afr. Invertebr. 48, 41–57.

Benninghoff, W.S., 1962. Calculation of pollen and spore density in sediments by addition of exotic pollen in known quantities. Pollen Spores 4, 332–333.

Blayden, I., 1984. The Newcastle Coal Measures – An alluvial fan sedimentary facies. In: Jones, B.G., Hutton, A.C. (Eds.), Fluvio-Deltaic Systems – Facies Analysis in Exploration. Australasian Sedimentologists Group Publication, Wollongong, NSW, pp. 63–89.

Bocking, M., Howes, M., Weber, C., 1988. Palaeochannel development in the Moon Island Beach Sub-Group of the Newcastle Coal Measures. In: Proceedings of the 22nd Symposium on Advances in the Study of the Sydney Basin. Department of Geology, University of Newcastle, NSW, pp. 37–45.

Bohacs, K., Suter, J., 1997. Sequence stratigraphic distribution of coaly rocks: fundamental controls and paralic examples. Am. Assoc. Pet. Geol. Bull. 81, 1612–1639. https://doi.org/10.1306/3B05C3FC-172A-11D7-8645000102C1865D.

Boyd, R., Little, M., Herbert, C., 1998. A new look at the Newcastle Coal Measures – Two contrasting approaches to their formation and sequence stratigraphy. In: Field Excursion Guidebook for the 32nd Symposium on Advances in the Study of the Sydney Basin. Department of Geology, University of Newcastle, NSW, pp. 1–51.

Bradley, G., 1993. A new tectonic and depositional model for the offshore Sydney Basin (NSW/P10). In: Proceedings of the 27th Symposium on Advances in the Study of the Sydney Basin. Department of Geology, University of Newcastle, NSW, pp. 19–26.

Brakel, A.T., Wilford, G.E., Totterdell, J.M., Bradshaw, M., 1995. Palaeogeographic settings of Australian coal measures. In: Ward, C.R., Harrington, H.J., Mallett, C.W., Beeston, J.W. (Eds.), Geology of Australian Coal Basins. Coal Geology Group Special Publication 1. Geological Society of Australia, Sydney, pp. 1–15.

Branagan, D.F., Johnson, M.W., 1970. Permian sedimentation in the Newcastle coalfield, New South Wales. Proceedings of the Australasian Institute of Mining and Metallurgy 235, 1–36.

Breckenridge, J., Maravelis, A., Catuneanu, O., Ruming, K., Holmes, E., Collins, W.J., 2019. Outcrop analysis and facies model of an Upper Permian tidally influenced fluvio-deltaic system: Northern Sydney Basin, SE Australia. Geol. Mag. 156, 1715–1741. https://doi.org/10.1017/S0016756818000973.

Bridge, J.S., 2003. Rivers and Floodplains: Forms, Processes and Sedimentary Record. Blackwell Science, Oxford, 491 pp.

Bristow, C.S., Skelly, R.L., Ethridge, F.G., 1999. Crevasse splays from the rapidly aggrading, sand-bed, braided Niobrara River, Nebraska: effect of base-level rise. Sedimentology 46, 1029–1047. https://doi.org/10.1046/j.1365-3091.1999.00263.x.

Chalmers, G.R.L., Boyd, R., Diessel, C.F.K., 2013. Accommodation-based coal cycles and significant surface correlation of low-accommodation Lower Cretaceous coal seams, Lloydminster heavy oil field, Alberta, Canada: implications for coal quality distribution. Am. Assoc. Pet. Geol. Bull. 97, 1347–1369. https://doi.org/10.1306/12181211187.

Chapman, T., Milan, L.A., Metcalfe, I., Blevin, P.L., Crowley, J., 2022. Pulses in silicic arc magmatism initiate end-Permian climate instability and extinction. Nat. Geosci. 15, 411–416. https://doi.org/10.1038/s41561-022-00934-1.

Clarke, W.B., 1843. On a fossil pine forest in Kurrur-Kuran in the inlet of Awaaba, east coast of Australia. Proceedings of the Geological Society of London 4, 161–164.

Coal Resource Development Committee, 1994. Effects of Land Use on Coal Resources. New South Wales Department of Mineral Resources, Sydney, New South Wales.

Conolly, J.R., Ferm, J.C., 1971. Permo-Triassic sedimentation patterns, Sydney Basin, Australia. Am. Assoc. Pet. Geol. Bull. 55, 2018–2032. https://doi.org/10.1306/819A3DC0-16C5-11D7-8645000102C1865D.

Cowan, E.J., 1993. Longitudinal fluvial drainage patterns within a foreland basin-fill: Permo-Triassic Sydney Basin, Australia. Sediment. Geol. 85, 557–577. https://doi.org/10.1016/0037-0738(93)90102-B.

Creech, M., 2002. Tuffaceous deposition in the Newcastle Coal Measures: challenging existing concepts of peat formation in the Sydney Basin, New South Wales, Australia. Int. J. Coal Geol. 51, 185–214. https://doi.org/10.1016/S0166-5162(02)00084-8.

Creech, M., 2007. The Depositional Environment of the Newcastle Coal Measures: Insights from Tuffaceous Sedimentation, Tree Preservation and Long Distance Correlations. PhD thesis,. University of Newcastle, NSW (Unpublished), 323 pp.
Dai, S.F., Bechtel, A., Eble, C.F., Flores, R.M., French, D., Graham, I.T., Hood, M.M., Hower, J.C., Korasidis, V.A., Moore, T.A., Püttmann, W., Wei, Q., Zhao, L., O'Keefe, J.M.K., 2020. Recognition of peat depositional environments in coal: a review. Int. J. Coal Geol. 219, 103383, 67 pp. https://doi.org/10.1016/j.coal.2019.103383.
David, T.W.E., 1907. The Geology of the Hunter River Coal Measures, New South Wales. Memoir of the Geological Survey of New South Wales, Geology, 4, 453 pp.
de Jersey, N.J., 1962. Triassic spores and pollen grains from the Ipswich Coalfield. In: Geological Survey of Queensland Publications, 307, pp. 1–18.
Diessel, C.F.K., 1980. Newcastle and Tomago Coal Measures. In: Herbert, C., Helby, R. (Eds.), A Guide to the Sydney Basin, Geological Survey of New South Wales, Bulletin, vol. 26, pp. 101–114.
Diessel, C.F.K., 1984. Excursion Synopsis for Excursion 1, 18th Symposium on Advances in the Study of the Sydney Basin. Department of Geology, University of Newcastle, NSW, 34 pp.
Diessel, C.F.K., 1986. On the correlation between coal facies and depositional environments. In: Proceedings of the 20th Symposium on Advances in the Study of the Sydney Basin, Department of Geology, University of Newcastle, NSW, pp. 19–22.
Diessel, C.F.K., 1989. Excursion Guide. In: Proceedings of the 23rd Symposium on Advances in the Study of the Sydney Basin, Department of Geology, University of Newcastle, NSW, pp. 1–13.
Diessel, C.F.K., 1992. Coal-Bearing Depositional Systems. Springer-Verlag, Berlin, 721 pp.
Diessel, C.F.K., Moelle, K.H.R., 1988. Field Excursion Guide for the 22nd Newcastle Symposium. Department of Geology, University of Newcastle (NSW), 21 pp.
Diessel, C.F.K., Boyd, R., Wadsworth, J., Leckie, D., Chalmers, G., 2000. On balanced and unbalanced accommodation/peat accumulation ratios in the Cretaceous coals from Gates Formation, Western Canada, and their sequence-stratigraphic significance. Int. J. Coal Geol. 43, 143–186. https://doi.org/10.1016/S0166-5162(99)00058-0.
Duff, P.McL.D., 1967. Cyclic sedimentation in the Permian coal measures of New South Wales. J. Geol. Soc. Aust. 14, 293–307. https://doi.org/10.1080/00167616708728667.
Engel, B.A., 1966. Explanatory Notes on the Newcastle 1:250,000 Geological Sheet SI 56–2. Geological Survey of New South Wales, Sydney.
Evans, P.R., 1962. Palynological Examination of A.A.O. Westgrove No. 2 well, Surat Basin, Queensland, Well Completion Report. Mines Administration Pty Ltd.. Q/55-56P/11 0.
Farrell, K.M., 2001. Geomorphology, facies architecture, and high-resolution, non-marine sequence stratigraphy in avulsion deposits, Cumberland Marshes, Saskatchewan. Sediment. Geol. 139, 93–150. https://doi.org/10.1016/S0037-0738(00)00150-0.
Ferguson, R.J., Brierley, G.J., 1999. Levee morphology and sedimentology along the lower Tuross River, South-Eastern Australia. Sedimentology 46, 627–648. https://doi.org/10.1046/j.1365-3091.1999.00235.x.
Fielding, C.R., 1984. A coal depositional model for the Durham Coal Measures of NE England. J. Geol. Soc. Lond. 141, 919–931. https://doi.org/10.1144/gsjgs.141.5.0919.
Fielding, C.R., 1985. Coal depositional models and the distinction between alluvial and delta plain environments. Sediment. Geol. 42, 41–48. https://doi.org/10.1016/0037-0738(85)90072-7.
Fielding, C.R., 1986. Fluvial channel and overbank deposits from the Westphalian of the Durham coalfield, NE England. Sedimentology 33, 119–140. https://doi.org/10.1111/j.1365-3091.1986.tb00748.x.
Fielding, C.R., 1987. Coal depositional models for deltaic and alluvial plain sequences. Geology 15, 661–664. https://doi.org/10.1130/0091-7613(1987)15<661:CDMFDA>2.0.CO;2.
Fielding, C.R., Alexander, J., 2001. Fossil trees in ancient fluvial channel deposits: evidence of seasonal and longer-term climatic variability. Palaeogeogr. Palaeoclimatol. Palaeoecol. 170, 59–80. https://doi.org/10.1016/S0031-0182(01)00227-9.
Fielding, C.R., Falkner, A.J., Scott, S.G., 1993. Fluvial response to foreland basin overfilling; the Late Permian Rangal Coal Measures in the Bowen Basin, Queensland, Australia. Sediment. Geol. 85, 475–497. https://doi.org/10.1016/0037-0738(93)90099-Q.
Fielding, C.R., Alexander, J., Allen, J.P., 2018. The role of discharge variability in the formation and preservation of alluvial sediment bodies. Sediment. Geol. 365, 1–20. https://doi.org/10.1016/j.sedgeo.2017.12.022.
Fielding, C.R., Frank, T.D., McLoughlin, S., Vajda, V., Mays, C., Tevyaw, A.P., Winguth, A., Winguth, C., Nicoll, R.S., Bocking, M., Crowley, J.L., 2019. Age and pattern of the southern high-latitude continental end-Permian extinction constrained by multiproxy analysis. Nat. Commun. 10 (385), 12p. https://doi.org/10.1038/s41467-018-07934-z.
Fielding, C.R., Frank, T.D., Tevyaw, A.P., Savatic, K., Vajda, V., McLoughlin, S., Mays, C., Nicoll, R.S., Bocking, M., Crowley, J.L., 2021. Sedimentology of the continental end-Permian extinction event in the Sydney Basin, eastern Australia. Sedimentology 68, 30–62. https://doi.org/10.1111/sed.12782.
Fielding, C.R., Frank, T.D., Savatic, K., Mays, C., McLoughlin, S., Vajda, V., Nicoll, R.S., 2022. Environmental change in the late Permian of Queensland, NE Australia: the warmup to the end-Permian Extinction. Palaeogeogr. Palaeoclimatol. Palaeoecol. 594, 110936, 30 pp. https://doi.org/10.1016/j.palaeo.2022.110936.
Fielding, C.R., Frank, T.D., Birgenheier, L.P., 2023. A revised, late Palaeozoic glacial time-space framework for eastern Australia, and comparisons with other regions and events. Earth Sci. Rev. 236, 104263, 15pp. https://doi.org/10.1016/j.earscirev.2022.104263.
Fielding, C.R., Alexander, J., Argiro, A., 2025. Towards a new generation of fluvial facies models for the interpretation of ancient deposits, based on inter-annual peak discharge variance of modern rivers. Sedimentology 72, 275–329. https://doi.org/10.1111/sed.13234.
Filguera-Rivera, M., Smith, N.D., Slingerland, R.L., 2007. Controls on natural levée development in the Columbia River, British Columbia, Canada. Sedimentology 54, 905–919. https://doi.org/10.1111/j.1365-3091.2007.00865.x.
Flood, P.G., Brady, S.A., 1985. Origin of large-scale crossbeds in the Late Permian coal measures of the Sydney and Bowen Basins, eastern Australia. Int. J. Coal Geol. 5, 231–245. https://doi.org/10.1016/0166-5162(85)90026-6.
Foster, C.B., 1972. Spore-pollen assemblages of the Bowen Basin, Queensland (Australia): their relationship to the Permian-Triassic boundary. Reviews of Palaeobotany and Palynology 36, 165–183.
Foster, C.B., 1979. Permian plant microfossils of the Blair Athol Coal Measures, Baralaba Coal Measures, and basal Rewan Formation of Queensland. In: Geological Survey of Queensland Publications, 372, pp. 1–244.
Frank, T.D., Fielding, C.R., Winguth, A.M.E., Savatic, K., Tevyaw, A., Winguth, C., McLoughlin, S., Vajda, V., Mays, C., Nicoll, R., Bocking, M., Crowley, J.L., 2021. Pace, Magnitude, and nature of terrestrial climate change through the end-Permian extinction in southeastern Gondwana. Geology 49, 1089–1095.
Glasspool, I., 2000. A major fire event recorded in the mesofossils and petrology of the Late Permian, Lower Whybrow coal seam, Sydney Basin, Australia. Palaeogeogr. Palaeoclimatol. Palaeoecol. 164, 357–380. https://doi.org/10.1016/S0031-0182(00)00194-2.
Glen, R.J., 2005. The Tasmanides of eastern Australia. In: Vaughan, A.P.M., Leat, P.T., Pankhurst, R.J. (Eds.), Terrane processes at the margins of Gondwana, 246. Geological Society of London Special Publication, pp. 23–96.
Goldbery, R., Holland, W.N., 1973. Stratigraphy and sedimentation of redbed facies in Narrabeen Group of Sydney Basin, Australia. Am. Assoc. Pet. Geol. Bull. 57, 1314–1334. https://doi.org/10.1306/83D90EA8-16C7-11D7-8645000102C1865D.
Grevenitz, P., Carr, P., Hutton, A., 2003. Origin, alteration and geochemical correlation of Late Permian airfall tuffs in coal measures, Sydney Basin, Australia. Int. J. Coal Geol. 55, 27–46. https://doi.org/10.1016/S0166-5162(03)00064-8.
Gugliotta, M., Flint, S.S., Hodgson, D.M., Veiga, G.D., 2016. Recognition criteria, characteristics and implications of the fluvial to marine transition zone in ancient deltaic deposits (Lajas Formation, Argentina). Sedimentology 63, 1971–2001. https://doi.org/10.1111/sed.12291.
Hampson, G., 1995. Discrimination of regionally extensive coals in the Upper Carboniferous of the Pennine Basin, UK using high resolution sequence stratigraphic concepts. In: Whateley, M.K.G., Spears, D.A. (Eds.), European Coal Geology, 82. Geological Society of London Special Publication, pp. 79–97. https://doi.org/10.1144/GSL.SP.1995.082.01.04.
Harrington, H.J., Brakel, A.T., Hunt, J.W., Wells, A.T., Middleton, M.F., O'Brien, P.E., Hamilton, D.S., Beckett, J., Weber, C.R., Radke, S., Totterdell, J.M., Swaine, D.J., Schmidt, P.W., 1989. Permian Coals of Eastern Australia, 2. Bureau of Mineral Resources, Geology and Geophysics Australia, Bulletin, p. 231.
Hawley, S.P., Brunton, J.S., 1995. The Newcastle Coalfield: Notes to accompany the 1:100,000 Newcastle Coalfield Regional Geology Map. Geological Survey of New South Wales, Report GS1995/256, 89p.
Hawley, S.P., Glen, R.A., Baker, C.J., 1995. Newcastle Coalfield Regional Geology, 1:100,000 Map. New South Wales Department of Mineral Resources.
Helby, R., 1973. Review of Late Permian and Triassic Palynology of New South Wales, 4. Geological Society of Australia, Special Publication, pp. 141–155.
Herbert, C., 1980. Depositional environment of the Sydney Basin. In: Herbert, C., Helby, R. (Eds.), A Guide to the Sydney Basin, Geological Survey of New South Wales, Bulletin, vol. 26, pp. 10–52.
Herbert, C., 1997. Relative sea level control of deposition in the Late Permian Newcastle Coal Measures of the Sydney Basin, Australia. Sediment. Geol. 107, 167–187. https://doi.org/10.1016/S0037-0738(96)00027-9.
A Guide to the Sydney Basin. In: Herbert, C., Helby, R. (Eds.), Geol. Surv. NSW Bull. 26, 603.
Holcombe, R.J., Stephens, C.J., Fielding, C.R., Gust, D., Little, T.A., Sliwa, R., Kassan, J., McPhie, J., Ewart, A., 1997. Tectonic evolution of the northern New England Fold Belt: the Permian-Triassic Hunter-Bowen event. In: Ashley, P.M., Flood, P.G. (Eds.), Tectonics and Metallogenesis of the New England Orogen, 19. Geological Society of Australia Special Publication, pp. 52–65.
Huyskens, M.H., 2014. Improving precision and accuracy of U-Pb geochronology with application to the Permian period, PhD thesis. Australian National University, Canberra, ACT, p. 154.
İnci, U., 2002. Depositional evolution of Miocene coal successions in the Soma coalfield, western Turkey. Int. J. Coal Geol. 51, 1–29. https://doi.org/10.1016/S0166-5162(01)00066-0.
Ives, M., Brunton, J., Edwards, J., Rigby, R., Tobin, C., Weber, C.R., 1999. Revision of the stratigraphy of the Newcastle Coal Measures. In: Coalfield Geology Council of New South Wales Bulletin, 1, pp. 113–119.
Jell, P.A., 2004. The fossil insects of Australia. In: Memoirs of the Queensland Museum, 50, pp. 1–124.
Jerrett, R.M., Hodgson, D.M., Flint, S.S., Davies, R.C., 2011. Control of relative sea level and climate on coal character in the Westphalian C (Atokan) Four Corners Formation, central Appalachian Basin, U.S.A. J. Sediment. Res. 81, 420–445. https://doi.org/10.2110/jsr.2011.37.
Jones, J.G., Conaghan, P.J., McDonnell, K.L., 1987. Coal Measures of an orogenic recess: Late Permian Sydney Basin, Australia. Palaeogeogr. Palaeoclimatol. Palaeoecol. 58, 203–219. https://doi.org/10.1016/0031-0182(87)90060-5.

Jorgensen, P.J., Fielding, C.R., 1996. Facies architecture of alluvial floodbasin deposits: three-dimensional data from the Upper Triassic Callide Coal Measures of eastcentral Queensland, Australia. Sedimentology 43, 479–495. https://doi.org/10.1046/j.1365-3091.1996.d01-25.x.

Klootwijk, C., 2016. Paleomagnetism of the Carboniferous Rouchel Block, Tamworth Belt, and pole path revision for the New England Orogen, eastern Australia. Aust. J. Earth Sci. 63, 513–549. https://doi.org/10.1080/08120099.2016.1223170.

Kramer, W., Weatherall, G., Offler, R., 2001. Origin and correlation of tuffs in the Permian Newcastle and Wollombi Coal Measures, NSW, Australia, using chemical fingerprinting. Int. J. Coal Geol. 47, 115–135.

Kremenetski, K.V., Velichko, A.A., Borisova, A.K., MacDonald, G.M., Smith, L.C., Frey, K. E., Orlova, A., 2003. Peatlands of the West Siberian lowlands: current knowledge on zonation, carbon content and Late Quaternary history. Quat. Sci. Rev. 22, 703–723.

Lajoie, J., 1984. Volcaniclastic rocks. In: Walker, R.G. (Ed.), Facies Models, 2nd edition, Geoscience Canada Reprint Series 1. Geological Association of Canada, St John's, Newfoundland, pp. 39–52.

Laurie, J.R., Bodorkos, S., Nicoll, R.S., Crowley, J.L., Mantle, D.J., Mory, A.J., Wood, G. R., Backhouse, J., Holmes, E.K., Smith, T.E., Champion, D.C., 2016. Calibrating the middle and late Permian palynostratigraphy of Australia to the geologic time-scale via U–Pb zircon CA-IDTIMS dating. Aust. J. Earth Sci. 63, 701–730. https://doi.org/10.1080/08120099.2016.1233456.

Le Knight, O.M., 1950. Fossil insect beds of Belmont. In: N.S.W. Records of the Australian Museum, 22, pp. 251–253.

Li, Y.N., Shao, L.Y., Fielding, C.R., Wang, D.W., Mu, G.Y., Luo, H.H., 2020. Sequence stratigraphic analysis of thick coal seams in paralic environments – a case study from the Early Permian Shanxi Formation in the Anhe coalfield, Henan Province, North China. Int. J. Coal Geol. 222, 103451. https://doi.org/10.1016/j.coal.2020.103451.

Lindsay, G., Herbert, C., 2002. Coal and conglomerate in the Newcastle Coal Measures – coeval facies or temporally unrelated? Int. J. Coal Geol. 51, 169–184. https://doi.org/10.1016/S0166-5162(02)00083-6.

Little, M.P., 1998. Stratigraphic Analysis of the Newcastle Coal Measures, Sydney Basin, Australia. PhD thesis. University of Newcastle, NSW (Unpublished).

Loughnan, F.C., 1966. A comparative study of the Newcastle and Illawarra Coal Measure sediments of the Sydney Basin, New South Wales. J. Sediment. Petrol. 36, 1016–1025. https://doi.org/10.1306/74D715E6-2B21-11D7-8648000102C1865D.

Loughnan, F.C., Ray, A.S., 1978. The Reids Mistake Formation at Swansea, New South Wales. Journal of the Geological Society of Australia 25, 473–481.

Lovett, G.M., Cole, J.J., Pace, M.L., 2006. Is net ecosystem production equal to ecosystem carbon accumulation? Ecosystems 9, 152–155. https://doi.org/10.1007/s10021-005-0036-3.

Mackenzie, P.J., Britten, R.A., 1969. Newcastle Coal Measures. J. Geol. Soc. Aust. 16, 339–350.

Maravelis, A.G., Breckenridge, J., Ruming, K., Holmes, E., Amelin, Y., Collins, W.J., 2020. Re-assessing the Upper Permian stratigraphic succession of the Northern Sydney Basin, Australia, by CA-IDTIMS. Geosciences 10, 474. https://doi.org/10.3390/geosciences10110474.

Martini, I.P., 2006. The cold climate peatlands of the Hudson Bay Lowland, Canada: Brief overview of recent work. In: Martini, I.P., Martinez Cortizas, A., Chesworth, W. (Eds.), Peatlands: Evolution and Record of Environmental and Climatic Changes, Developments in Earth Surface Processes, 9. Elsevier Science, Amsterdam, pp. 53–84. https://doi.org/10.1016/S0928-2025(06)09003-1.

Mayne, S.J., Nicholas, E., Bigg-Wither, A.L., Rasidi, J.S., Raine, M.J., 1974. Geology of the Sydney Basin – a review. Bur. Min. Res. Geol. Geophys. Bull. 149, 229 pp.

Mays, C., McLoughlin, S., 2022. End-Permian burnout: the role of Permian-Triassic wildfires in extinction, carbon cycling and environmental change in eastern Gondwana. Palaios 37, 292–317. https://doi.org/10.2110/palo.2021.051.

Mays, C., Vajda, V., Frank, T., Fielding, C., Nicoll, R.S., Tevyaw, A., McLoughlin, S., 2020. Refined Permian-Triassic floristic timeline reveals early collapse and delayed recovery of south polar terrestrial ecosystems. GSA Bull. 132, 1489–1513. https://doi.org/10.1130/B35355.1.

Mays, C., Vajda, V., McLoughlin, S., 2021. Permian–Triassic non-marine algae of Gondwana—distributions, natural affinities and ecological implications. Earth Sci. Rev. 212, 103382, 29 pp. https://doi.org/10.1016/j.earscirev.2020.103382.

Mays, C., Amores, M., Mays, A., 2025. Field-of-view subsampling: a novel 'exotic marker' method for absolute abundances, validated by simulation and microfossil case studies. PLoS One. https://doi.org/10.1371/journal.pone.0320887.

McCabe, P.J., 1991. Tectonic controls on coal accumulation. Bull. Geol. Soc. Fr. 162, 277–282.

McDougall, I., Maboko, M.A.H., Symonds, P.A., McCulloch, M.T., Williams, I.S., Kudrass, H.R., 1994. Dampier Ridge, Tasman Sea, as a stranded continental fragment. Aust. J. Earth Sci. 41, 395–406. https://doi.org/10.1080/08120099408728150.

McLoughlin, S., 1990. Palaeobotany and Palaeoenvironments of Permian Strata, Bowen Basin, Queensland. PhD thesis. University of Queensland, Brisbane, 312 pp. (unpublished).

McLoughlin, S., Maksimenko, A., Mays, C., 2019. A new high-paleolatitude permineralized peat flora from the late Permian of the Sydney Basin, Australia. Int. J. Plant Sci. 180, 513–539. https://doi.org/10.1086/702939.

McMinn, A., 1987. Palynostratigraphy of the Stroud-Gloucester Trough, N.S.W. Alcheringa 11, 151–164. https://doi.org/10.1080/03115518708618986.

Melehan, S., Botziolis, C., Maravelis, A., Catuneanu, O., Ruming, K., Holmes, E., Collins, W.J., 2021. Sedimentology and stratigraphy of an Upper Permian sedimentary succession: Northern Sydney Basin, southeastern Australia. Geosciences 11, 273, 28 pp. https://doi.org/10.3390/geosciences11070273.

Metcalfe, I., Crowley, J.L., Nicoll, R.S., Schmitz, M., 2015. High-precision U-Pb CA-TIMS calibration of Middle Permian to Lower Triassic sequences, mass extinction and extreme climate-change in eastern Australian Gondwana. Gondwana Res. 28, 61–81. https://doi.org/10.1016/j.gr.2014.09.002.

Naylor, M., Sinclair, H.D., 2008. Pro- versus retro-foreland basins. Basin Res. 20, 285–303.

Nicoll, R.S., Bocking, M., Smith, T.E., Crowley, J.L., Bodorkos, S., Holmes, E.K., Mantle, D., Wood, G.R., 2017. Dating of marine incursions and unconformities in the Sydney and Gunnedah Basins of New South Wales using U-Pb zircon CA-IDTIMS dating of intercalated tuffs. Coalfield Geology Council of New South Wales, Newcastle, New South Wales.

Pace, M.L., Lovett, G.M., 2021. Primary production: The foundation of ecosystems. In: Weathers, K.C., Strayer, D.L., Likens, G.E. (Eds.), Fundamentals of Ecosystem Science, 2nd ed. Academic Press, London, pp. 29–53. https://doi.org/10.1016/B978-0-12-812762-9.00002-2.

Perez-Arlucea, M., Smith, N.D., 1999. Depositional patterns following the 1870s avulsion of the Saskatchewan River (Cumberland Marshes, Saskatchewan, Canada). J. Sediment. Res. 69, 62–73. https://doi.org/10.2110/jsr.69.62.

Pigg, K.B., McLoughlin, S., 1997. Anatomically preserved *Glossopteris* leaves from the Bowen and Sydney basins, Australia. Rev. Palaeobot. Palynol. 97, 339–359. https://doi.org/10.1016/S0034-6667(97)00007-9.

Potonié, R., 1960. Synopsis der Gattungen der Sporae dispersae. III. Teil: Nachträge Sporites, Fortsetzung Pollenites. Mit Generalregister zu Teil I–III, 189 pp.

Price, P.L., 1983. A Permian palynostratigraphy for Queensland. In: anonymous (Ed.), Permian Geology of Queensland. Geological Society of Australia, Queensland Division, Brisbane, pp. 155–212.

Price, P.L., 1997. Permian to Jurassic palynostratigraphic nomenclature of the Bowen and Surat basins. In: Green, P.M. (Ed.), The Surat and Bowen Basins, Southeast Queensland. Queensland Department of Mines and Energy, Brisbane, pp. 137–178.

Read, J., Francis, J., 1992. Responses of some Southern Hemisphere tree species to a prolonged dark period and their implications for high-latitude Cretaceous and Tertiary floras. Palaeogeogr. Palaeoclimatol. Palaeoecol. 99, 271–290. https://doi.org/10.1016/0031-0182(92)90019-2.

Retallack, G.J., Veevers, J.J., Morante, R., 1996. Global coal gap between Permian-Triassic extinction and Middle Triassic recovery of peat-forming plants. Bull. Geol. Soc. Am. 108, 195–207.

Roche, O., Azzaoui, N., Guillin, A., 2021. Discharge rate of explosive volcanic eruption controls runout distance of pyroclastic density currents. Earth Planet. Sci. Lett. 568, 117017. https://doi.org/10.1016/j.epsl.2021.117017.

Rosenbaum, G., 2018. The Tasmanides: Phanerozoic tectonic evolution of eastern Australia. Annual Reviews of Earth and Planetary Science 46, 291–325.

Rowe, H., Hughes, N., Robinson, K., 2012. The quantification and application of handheld energy-dispersive x-ray fluorescence (ED-XRF) in mudrock chemostratigraphy and geochemistry. Chem. Geol. 234-235, 122–131. https://doi.org/10.1016/j.chemgeo.2011.12.023.

Shao, L.Y., Zhang, P.F., Gayer, R.A., Chen, J.L., Dai, S.F., 2003. Coal in a carbonate sequence stratigraphic framework: the Upper Permian Heshan Formation in Central Guangxi, southern China. J. Geol. Soc. Lond. 160, 285–298. https://doi.org/10.1144/0016-764901-108.

Shi, G.R., Waterhouse, J.B., McLoughlin, S., 2010. The Lopingian of Australasia: a review of biostratigraphy, correlations, palaeogeography and palaeobiogeography. Geol. J. 45, 230–263. https://doi.org/10.1002/gj.1213.

Stancliffe, R.P.W., Sarjeant, W.A.S., 1994. The acritarch genus *Veryhachium* Deunff 1954, emend. Sarjeant and Stancliffe 1994: a taxonomic restudy and a reassessment of its constituent species. Micropaleontology 40, 223–241. https://doi.org/10.2307/1485817.

Stockmarr, J., 1971. Tablets with spores used in absolute pollen analysis. Pollen Spores 13, 615–621.

Stricanne, L., Munnecke, A., Pross, J., Servais, T., 2004. Acritarch distribution along an inshore–offshore transect in the Gorstian (lower Ludlow) of Gotland, Sweden. Rev. Palaeobot. Palynol. 130, 195–216. https://doi.org/10.1016/j.revpalbo.2003.12.007.

Suarez-Ruiz, I., Flores, D., Mendonca Filho, J.C., Hackley, P.C., 2012. Review and update of the applications of organic petrology: part 1, Geological applications. Int. J. Coal Geol. 99, 54–112. https://doi.org/10.1016/j.coal.2012.02.004.

Torsvik, T.H., Cocks, L.R.M., 2013. Gondwana from top to base in space and time. Gondwana Res. 24, 999–1030. https://doi.org/10.1016/j.gr.2013.06.012.

Tyson, R.V., 1995. Sedimentary Organic Matter: Organic Facies and Palynofacies. Chapman & Hall, London, 615 pp.

Underwood, J.R., Lambert, W., 1974. Centroclinal cross strata, a distinctive sedimentary structure. J. Sediment. Petrol. 44, 1111–1113. https://doi.org/10.1306/212F6C44-2B24-11D7-8648000102C1865D.

Vajda, V., McLoughlin, S., Mays, C., Frank, T., Fielding, C.R., Tevyaw, A., Lehsten, V., Bocking, M., Nicoll, R.S., 2020. End-Permian (252 Mya) deforestation, wildfires and flooding—an ancient biotic crisis with lessons for the present. Earth Planet. Sci. Lett. 529, 115875. https://doi.org/10.1016/j.epsl.2019.115875.

Van Asselen, S., 2011. The contribution of peat compaction to total basin subsidence: implications for the provision of accommodation space in organic-rich deltas. Basin Res. 23, 239–255. https://doi.org/10.1111/j.1365-2117.2010.00482.x.

van de Schootbrugge, B., Koutsodendris, A., Taylor, W., Weston, F., Wellman, C., Strother, P.K., 2023. Recognition of an extended record of euglenoid cysts: Implications for the end-Triassic mass extinction. Rev. Palaeobot. Palynol. 322, 105043. https://doi.org/10.1016/j.revpalbo.2023.105043.

van Soelen, E.E., Twitchett, R.J., Kürschner, W.M., 2018. Salinity changes and anoxia resulting from enhanced run-off during the late Permian global warming and mass extinction event. Clim. Past 14, 441–453. https://doi.org/10.5194/cp-14-441-2018.

Veevers, J.J., 2006. Updated Gondwana (Permian–Cretaceous) earth history of Australia. Gondwana Res. 9, 231–260. https://doi.org/10.1016/j.gr.2005.11.005.

Warbrooke, P.R., 1981. Depositional Environments of the Upper Tomago and Lower Newcastle Coal Measures, New South Wales. PhD thesis,. University of, Newcastle, NSW.
Warbrooke, P.R., 1984. Coal forming environments in the Greta, Tomago and Newcastle Coal Measures. In: Proceedings of the 18th Symposium on Advances in the Study of the Sydney Basin, Department of Geology, University of Newcastle, NSW, pp. 35–42.
Warbrooke, P.R., 1987. Depositional and chemical environments in Permian coal forming swamps from the Newcastle area. In: Proceedings of the 21st Symposium on Advances in the Study of the Sydney Basin, Department of Geology, University of Newcastle, NSW, pp. 1–10.
Ward, C.R., 1972. Sedimentation in the Narrabeen Group, southern Sydney Basin, New South Wales. J. Geol. Soc. Aust. 19, 393–409. https://doi.org/10.1080/00167617208728809.
Warren, A., 1997. A tetrapod fauna from the Permian of the Sydney Basin. Rec. Aust. Mus. 49, 25–33. https://doi.org/10.3853/j.0067-1975.49.1997.297.
Wei, W., Algeo, T.J., 2020. Elemental proxies for paleosalinity analysis of ancient shales and mudrocks. Geochim. Cosmochim. Acta 287, 341–366.
Willcox, J.B., Sayers, J., Stagg, H.M.J., van de Beuque, S., 2001. Geological framework of the Lord Howe Rise and adjacent ocean basins. In: Hill, K.C., Bernecker, T. (Eds.), Eastern Australasian Basin Symposium 2001: A Refocussed Energy Perspective for the Future. Petroleum Exploration Society of Australia Special Publication, pp. 211–225.
Zakharikhina, L.V., 2014. The rate of peat accumulation in the Holocene in Kamchatka. Eur. Soil Sci. 47, 556–561. https://doi.org/10.1134/S106422931406012X.
Zavattieri, A.M., Gutiérrez, P.R., Monti, M., 2020. Middle Triassic freshwater green algae and fungi of the Puesto Viejo Basin, Central-Western Argentina: palaeoenvironmental implications. Alcheringa 44, 430–459. https://doi.org/10.1080/03115518.2020.1749302.

SUPPLEMENTARY DATA FILES

Supplementary Fig. 1. Representative plant fossils from the Newcastle Coal Measures, northern

Sydney Basin: sphenopsids (A–G), ferns (H), glossopterid leaves (I O), glossopterid leaves with insect herbivory scars (P, Q), glossopterid reproductive organs (R–U). A, *Phyllotheca australis* Brongniart with multiple leaf whorls, Newcastle, AMF14246. B, *Phyllotheca australis* Brongniart, Newcastle, AMF6439. C, *Lelstotheca robusta* (Feistmantel) Maheshwari, Newcastle, AMF30078. D, *Raniganjia bengalensis* (Rigby) Pant & Nautiyal, Newcastle, AMF39534. E, *Phyllotheca etheridgei* Arber, Newcastle, AMF50940. F, *Schizoneura gondwanensis* Feistmantel, Newcastle, AMF38579. G, *Paracalamites australis* Rigby, in outcrop at Merewether Head. H, *Neomariopteris lobifolia* (Morris) Maithy, Newcastle, AMF1536. I, *Glossopteris browniana* Brongniart, Newcastle, AMF1932. J, *Glossopteris* sp. cf. *G. schopfii* Pigg, Newcastle, AMF26130. K, *Glossopteris xiphophylla* McLoughlin, Newcastle, AMF26130. L, *Glossopteris linearis* McCoy, Booraloo Subgroup, Belmont, AMF48110. M, *Glossopteris ampla* Dana, in outcrop above Nobbys Seam, Little Redhead. N, *Glossopteris plumate* McLoughlin, Booraloo Subgroup, Belmont, AMF48112. O, *Glossopteris burngrovensis* McLoughlin, Newcastle, AMF57341. P, *Glossopteris browniana* Brongniart with extensive margin-feeding insect damage, Booraloo Subgroup, Belmont, AMF46508. Q, *Glossopteris* sp. with deeply scalloped margin-feeding insect attack, Bahtahbah Gully, Booraloo Subgroup, Belmont, AMF128464. R, *Karingbalia inglisensis* (McLoughlin) McLoughlin, Newcastle, AMF37390. S, *Dictyopteridium* sp., Newcastle, AMF26130. T, *Lidgettonia belmontensis* (White), Belmont insect beds, Booraloo Subgroup, Belmont, AMF46525. U, *Rigbya* sp. Newcastle Coal Measures, Newcastle, AMF29086. All specimens in Australian Museum collections. All scale bars = 10 mm.

Supplementary Fig. 2. Plant fossils in coastal outcrops of the Newcastle Coal Measures, northern Sydney Basin. A, Autumnal leaf mat of *Noeggerathiopsis hislopii* (Bunbury) Feistmantel and *Glossopteris browniana* Brongniart; facies association B, above Dudley Seam, coastal cliffs at Merewether. B, Vertical and oblique segmented *Vertebraria australis* (glossopterid) roots extending from the base of the Upper Pilot Seam (facies C1) through 30-cm-thick tuff layer with convolutions (facies D1); Illawong Park, south of Swansea Heads. C, In situ upright sideritized glossopterid stump encased in lower part of Nobbys Tuff, Little Redhead; hammer = 280 mm long. D, In situ upright coalified stems extending upward from top of coal seam (facies C1) through base of Nobbys Tuff at Glenrock Lagoon; 360 mm of measuring tape visible. E, Inclined upright sideritized axis in facies association B flat-laminated siltstones to weakly cross-bedded sandstones; above Nobbys Tuff, Little Redhead; lens cap = 49 mm. F, Variably orientated woody debris on bedding plane in silicified tuff (facies D1) below Pilot Seam; Illawong Park, south of Swansea Heads; lens cap = 49 mm.

Supplementary Table 1. Relative and absolute abundances of palynofacies and palynomorph groups for the northern Sydney Basin outcrops of the Newcastle Coal Measures, New South Wales, Australia. All relative data are expressed as percentages, which are calculated as a proportion of the total for the respective count type (palynofacies count or palynomorph count). The targets of the absolute abundance estimates were the terrestrial organic microfossils (TOMs). The markers for these estimates were *Lycopodium* spores introduced into the assemblages during sample preparation (see the ‘materials and methods' section). Two measures of absolute abundances are provided; the ‘linear method’ and the ‘field-of-view subsampling method’ (FOVS

method, sensu Mays et al., 2025). AOM = (non-resinous) amorphous organic matter; all other abbreviations and statistical terms follow Mays et al. (2025). Taxa designated as ‘other probable freshwater algae/acritarchs' follow Mays et al. (2021).

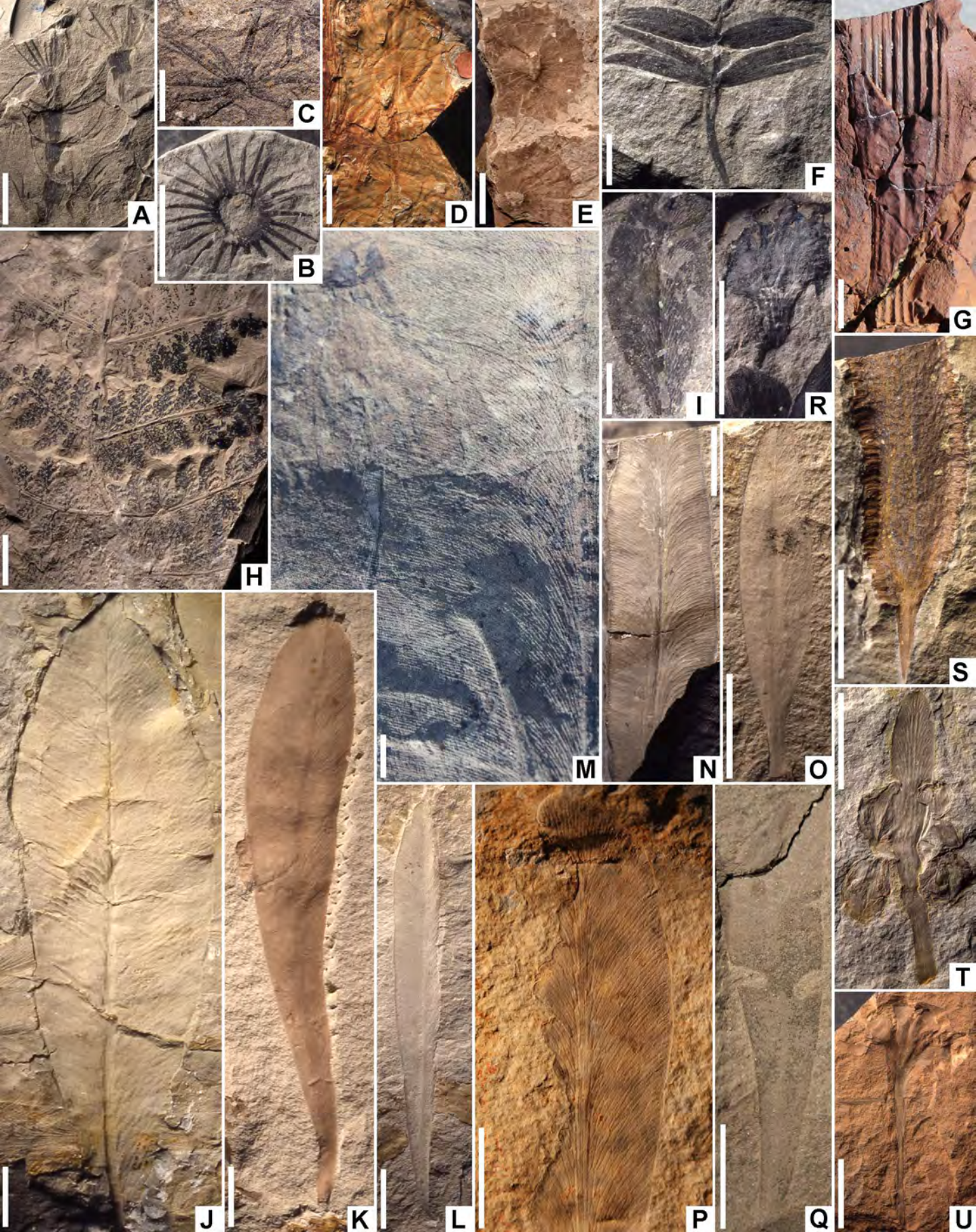
A
C
B
D
E
F
G
H
M
I
R
N
O
S
J
K
L
P
Q
T
U

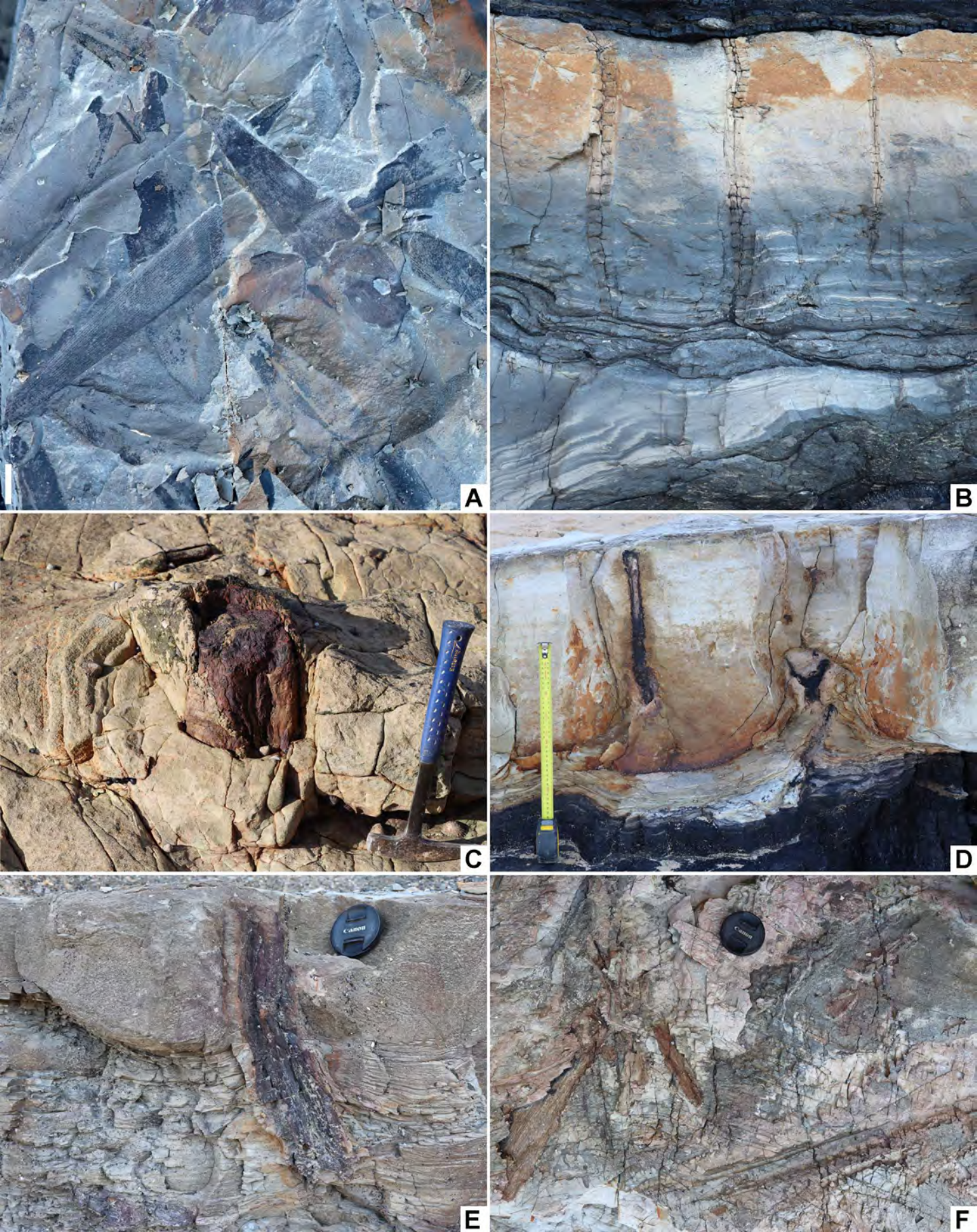
A
B
C
D
E
F

| Palynofacies counts | | |